Impacts of the Great Salt Lake on Summer Ozone Concentrations Along the Wasatch Front

Principal Investigator: Professor John Horel
(801) 581-7091
john.horel@utah.edu
Department of Atmospheric Sciences, University of Utah
135 S 1460 E, Rm 819
Salt Lake City, UT 84112-0110

Project Period: 1 July 2021- 31 December 2022

Report Submitted: 24 March 2023

Aerial view of the wetlands at the southern end of Farmington Bay

Executive Summary

We examined the meteorological factors contributing to elevated ozone concentrations along the southeastern margins of the Great Salt Lake that may serve as a source region for high ozone concentrations along the Wasatch Front. Multiple factors were hypothesized to contribute to elevated ozone in the Farmington Bay region: (1) ozone precursors from the urban corridor (NOx and VOCs) and local biogenic precursors near freshwater ponds are transported by the nocturnal land breeze over the playa surfaces; (2) actinic fluxes are elevated due to the high albedo over exposed playa surfaces; (3) initial development of the lake breeze concentrates precursors and ozone within the relatively shallow stable lake boundary layer; and (4) the lake breeze then transports ozone into the nearby urban regions later in the afternoon.

This study tied directly to the overarching goals of the Science for Solutions program to improve understanding of summertime ozone pollution along the Wasatch Front. The primary foci for this study were Priority I- Source Contributions to Summer-Time Ozone and Priority V- Air Exchange Processes and Pollutants Mass Transport. We examined summer ozone exceedances exacerbated by emission sources and processes near the Farmington Bay region and how air mass exchanges affect the transport of ozone and its precursors.

Our hypotheses were addressed using existing observations in Salt Lake and Davis counties during the 2015-2022 summers. Additional sensors were deployed during summer 2022 to fill gaps in critical locations that have not been sampled adequately before. The core task for this project was to evaluate from ozone observations and meteorological observations the timing of buildup in ozone in the southern Farmington Bay region and subsequent transport into Davis and Salt Lake counties.

Summer 2017 had the highest ozone concentrations across Davis and Salt Lake counties during the 2015-2022 period. The number of ozone exceedance events during summer 2021 were nearly as high as those during 2017 in part as a result of nearby and distant wildfires. The number of exceedances at stations in Davis and Salt Lake counties during summer 2022 were near the median of such events during the 2015-2022 period with limited impacts from wildfires.

The diurnal evolution of high ozone events in the Farmington Bay region during summer 2022 have many features in common: high ozone titration overnight followed by very rapid increases during morning hours; and generally quiescent synoptic meteorological conditions such that local thermally-forced circulations dominate. Down-valley flows overnight extend through metropolitan Salt Lake County and often extend across the wetlands south of Farmington Bay. Downslope flows through the less-urbanized Weber and Davis population centers extend southwestward and westward respectively into Farmington Bay. Flows reverse to up-valley through the Salt Lake Valley and eastward in Weber and Davis counties during late morning/early afternoon coinciding with maximum ozone increases. Lake breezes often develop from Gilbert Bay and then extend eastward across the Salt Lake Airport region and southeastward into the Salt Lake Valley.

Enhanced actinic fluxes due to increased albedo of exposed playa surfaces in the Farmington Bay region do not appear to be related to enhanced increases in ozone concentrations. Characteristics of the playa surfaces (wetness, soil type, etc.) affect total shortwave and ultraviolet radiation albedo. Playa surfaces have substantively lower albedo after rainstorms. There is no strong connection between the times when higher peak ozone concentrations were observed and when playa surfaces were dry with higher surface albedos during the summer of 2022. Since our site on the playa was furthest from major point and mobile sources of NOx and VOC emissions, it is not surprising that ozone concentrations there tended to be lower even though the underlying surface was more reflective in that region.

We intend to continue examining the data collected as part of this study. Provisional data and figures are available via the link: https://home.chpc.utah.edu/~u1375211/o3_2022/.
The data and results from this study should be of great utility for future studies of summer ozone along the Wasatch Front. We have demonstrated the utility of the data available from the operational Terminal Doppler Weather Radar and research deployments of surface based remote sensors (sodars, ceilometers) to examine the impacts of complex boundary layer flows on transport of chemical species affecting ozone along the Wasatch Front.

Future field programs intended to inform State Implementation Plans required for ozone exceedances along the Wasatch Front should recognize the need to monitor conditions both continuously throughout the summer season and during intensive field periods that take advantage of a range of instrumentation. The interplay between emission sources and photochemical production and destruction of ozone is modulated extensively by a rich mix of boundary layer processes spanning a wide range of temporal and spatial scales. Considerable in-situ and remote observational assets are available that can be used to understand the coupling between atmospheric conditions and chemical processes and to initialize and validate models used to test strategies required for State Implementation Plans.

Background and Significance

The Wasatch Front experiences exceedances of the National Ambient Air Quality Standard (NAAQS) for ozone during summer due to a complex mix of local and remote photochemical processes. The 2015 Great Salt Lake Summer Ozone Study that was supported by the Division of Air Quality was a small, yet the most comprehensive, field campaign to understand ozone concentrations in the vicinity of the Great Salt Lake (Horel et al. 2016a, b). The 2015 Summer Ozone Study identified that the Farmington Bay region was potentially a source region for high ozone concentrations in Davis and Salt Lake counties but did not fully explain why that may be the case. Figure 1 summarizes the variations in ozone concentrations during 16-30 June 2015 when ozone concentrations were high around the Great Salt Lake and along the Wasatch Front (Long 2016). Nighttime land breezes carry low ozone concentrations towards the lake while afternoon lake breezes transport much higher ozone concentrations towards the urban corridor. The concentrations during the afternoon at Bountiful (QBV), SaltAir (QSA), and the temporary site O3SO2 were consistently some of the highest during the field campaign. Ozone concentrations in those areas built up rapidly in the late morning. Based on observational data and modeling, Blaylock et al. (2017a) provided a detailed examination of how a lake breeze front contributes to transport of high concentrations of ozone from the Farmington Bay region southward throughout the Salt Lake Valley.

We hypothesized that multiple factors contribute to elevated ozone in the southern Farmington Bay region: (1) ozone precursors from the urban corridor (NOx and VOCs) and local biogenic precursors near freshwater ponds are transported by the nocturnal land breeze over the playa surfaces; (2) actinic fluxes are elevated due to the high albedo over exposed playa surfaces; (3) initial development of the lake breeze concentrates precursors and ozone within the relatively shallow stable lake boundary layer; and (4) the lake breeze then transports ozone into the nearby urban regions later in the afternoon. VOC precursor emission sources likely include the refineries nearby in North Salt Lake.

Figure 2 summarizes NOX and VOC emissions for Davis and Salt Lake counties from the Northern Wasatch Front 2017 Summertime Emissions Inventory estimated for 5 July 2017, a weekday with high ozone concentrations and record high temperatures over 40^{o}C (https://home.chpc.utah.edu/~u0864163/OZONE_public/NWF-SMOKE-Summary-Report.html). Vehicles and solvents are the leading sources for NOX and VOCs, respectively, in both counties with substantively higher emissions from Salt Lake than Davis. The emissions inventory was derived without considering chemical interactions or meteorological impacts. For context for our later results, Figure 3 illustrates the interplay between emissions, chemical reactions, and meteorology at Bountiful (QBV), Davis County on 5 July 2017. Relatively weak easterly winds after midnight transported moderate levels of background ozone downslope that underwent titration with the lowest concentrations observed at sunrise. Concentrations peaked during this hot afternoon when winds were directed from the Farmington Bay region towards Bountiful. Strong easterly downslope winds that evening brought relatively high background ozone concentrations downward into the metropolitan area.

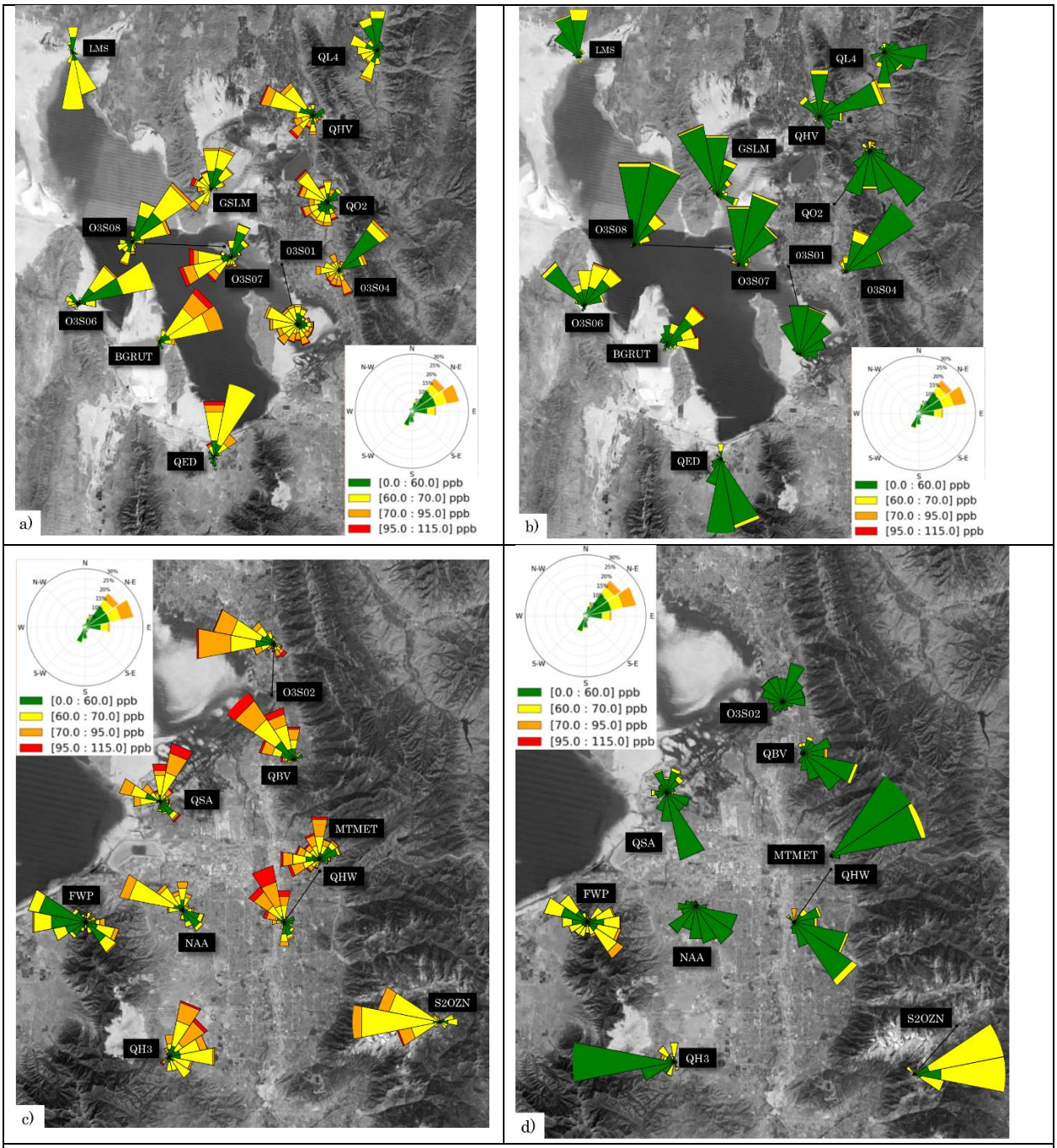

Figure 1. (a and c) Daytime (8 AM – 8 PM) ozone wind roses for 16-30 June 2015. The length of each of the 16 cardinal direction colored wedges represents the percentage of time the ozone concentrations fall within each colored range when the wind is blowing from that direction. (b and d) Nighttime (8PM-8AM) ozone wind roses. From Long (2016)

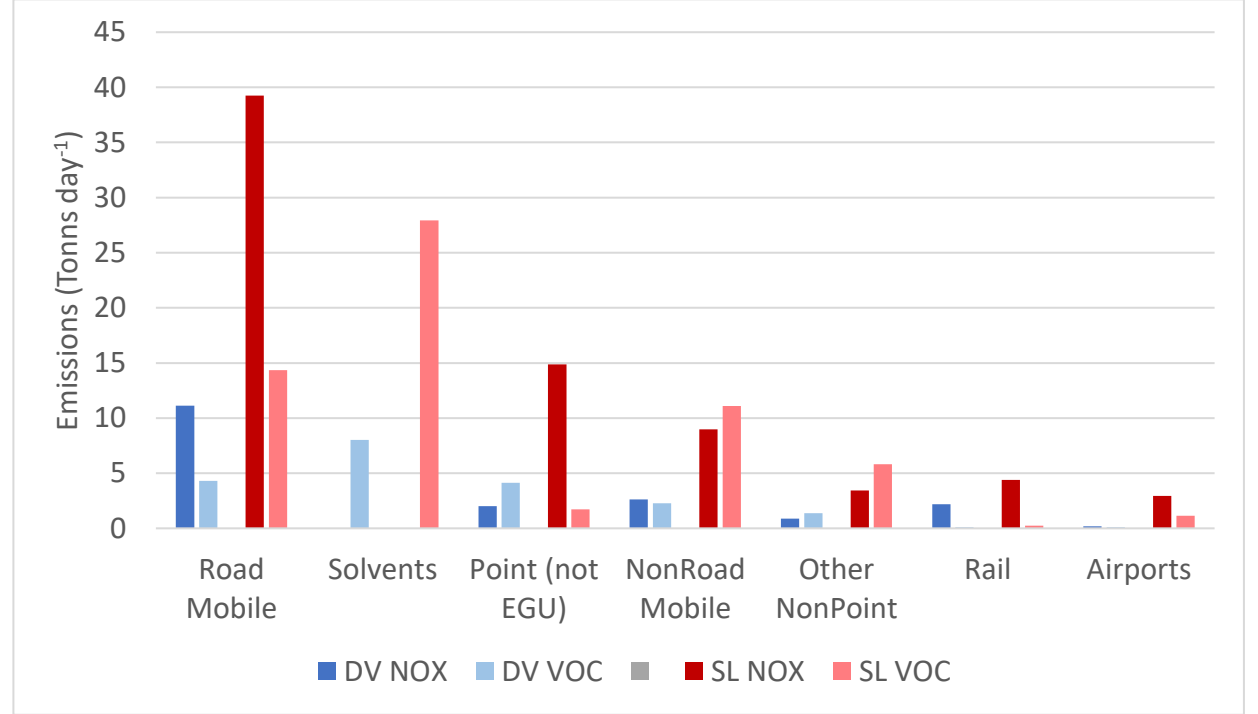

Figure 2. NOx and VOC emissions inventory for Davis (DV) and Salt Lake (SL) Counties from the Northern Wasatch Front 2017 Summertime Emissions Inventory.

The remainder of this report is subdivided into sections beginning with examination of summer ozone concentrations in the Farmington Bay region during 2015-2020 and followed by more in-depth analysis of the conditions during summer 2021 and 2022. That includes representative case studies during both summers, description of data assets deployed during summer 2022, and results pertaining to the hypotheses on the role of thermally-driven circulations and reflective underlying surfaces. Data Management for the information collected from the study follows.

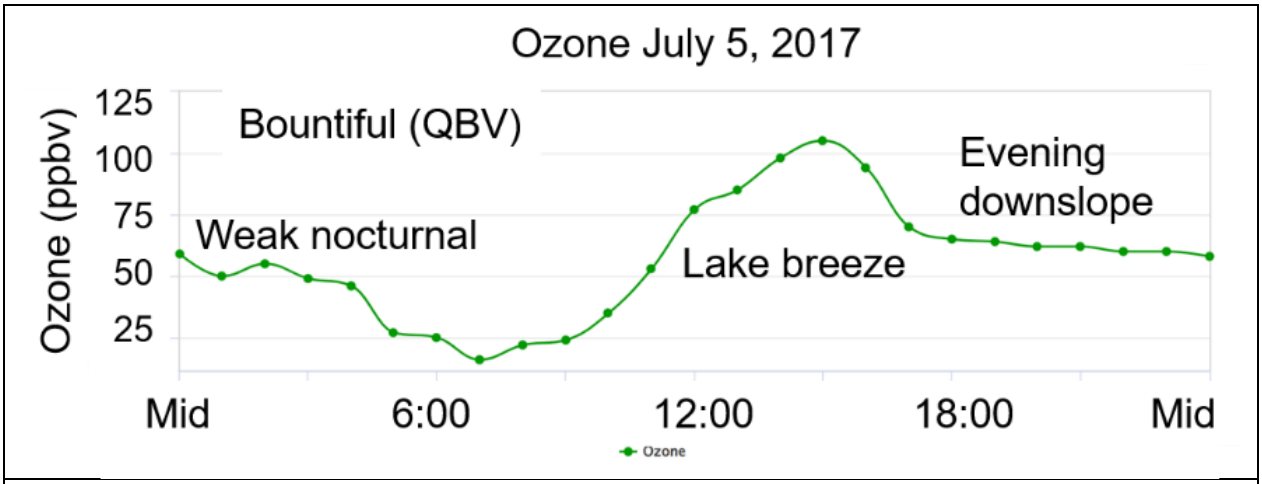

Figure 3. Evolution of hourly ozone concentrations at Bountiful on 5 July 2017.

The personnel participating in this study are as follows:

Personnel	Level	Responsibilities
John Horel	PI	Project management and data analysis
Sebastian Hoch	CoI	Deployment of sensors on Farmington Bay playa
Alexander Jacques	Staff	Data acquisition and analysis
Colin Johnson	Staff	Management of field equipment and analysis
Aaron McCutchan	Graduate Student	Analysis of TDWR radar imagery
Nicholas Buckley	Undergraduate	Assist installation of field equipment
Nadine Gabriel	Undergraduate	Examine ozone 2015-2020
Ashlynn Searer	Undergraduate	Analyze 2021 ozone
Samuel Jurado	Undergraduate	Analyze ozone
Alejandra Garcia	Undergraduate	Analyze 2022 ozone

1. Ozone Concentrations during 2015-2020 Summer Seasons

a) Background

To provide a baseline for understanding ozone concentrations during the 2021 and 2022 summer seasons, the previous six summer seasons (2015-2020) were examined to identify periods of high ozone concentrations for several sites near the Farmington Bay region and in the northern portion of Salt Lake County. Data acquisition and methodologies described in this section were then also applied to ozone concentration data collected during the 2021 and 2022 summer seasons.

b) Data and Methodology

Ozone concentration observations were acquired through observation data API Services made available from Synoptic Data PBC. For the 2015-2020 summer seasons, provisional observations from Utah Division of Air Quality sites located in Bountiful (site QBV) and Hawthorne Elementary School in Salt Lake City (site QHW) were accessed, as well as data from a Federal Equivalent Method (FEM) 2B Technologies 205 Ozone Monitor located on the University of Utah campus near the entrance of Red Butte Canyon (site MTMET). Starting with the 2018 summer season, observations from a new Utah Division of Air Quality site located in Rose Park (site QRP) were also added to this analysis, as Rose Park is often impacted by the thermally-

driven flows common to the region. Concentrations for each summer season were acquired for the time period of 1 June to 15 September in order to capture potential late summer season ozone exceedance episodes.

For each location and year, the ozone concentration dataset was reviewed, and any instances of clearly erroneous data were removed. The time series data from MTMET were transformed into hourly averaged time series to better align with the hourly averages produced by the Utah DAQ sites, as the nominal data reporting frequency of MTMET was every 5 minutes. An 8-hour averaged time series was then constructed from each hourly time series to align with the NAAQS for ozone.

Both the 1-hour and 8-hour time series per station per year were run through a series of statistical algorithms. For each calendar day, several ozone concentration percentiles (0, 25, 50, 75, 90, 100) were computed. Additionally, calendar days were logged if a particular site reached a maximum ozone concentration greater than several different thresholds (55, 60, 65, 70, 85, and 105 ppbv) to summarize occurrences of high ozone concentrations.

c) Results and Implications

Tables 1 and 2 provide the percentage of summer days sampled each year where the four sites eclipsed thresholds of ozone for 8-hour and 1-hour averages respectively. In summary, a median 11-15% of summer days each year surpassed the current 8-hour average NAAQS standard of greater than 70 ppbv. This translates to about 10-14 days each summer season (June-July-August). However, there can be large variability from season to season, as the summer of 2017 had over 20% of days surpassing the NAAQS standard for ozone at all four sites.

Any lowering of the current NAAQS standard from 70 to 65 or 60 ppbv would result in significant increases of occurrences where such new standards would be surpassed. The median percentage of days in violation of the standard increases to over 20% if the standard was 65 ppbv based on past data and would increase to well over one-third of the summer season if lowered to 60 ppbv. This scenario is illustrated in Figure 4 which shows the daily maximum 8-hour average ozone concentration for Bountiful (QBV) during the summer of 2020, where there are several instances falling short of the current NAAQS standard (70 pbbv - orange dashed line) but surpassing 60 or 65 ppbv.

Statistical occurrences were also computed using 1-hour averages in order to better understand high ozone event occurrences that might not be adequately captured by the current NAAQS standard of 8-hour averages, particularly given the large diurnal variability of ozone in this region due to urban titration that typically occurs overnight. Table 2 provides a similar summary to Table 1 but instead for hourly averages. In particular, it is noticeable that hourly ozone concentrations surpass 70 ppbv for 20-32% of days during the summer, which implies that even if the current NAAQS standard on an 8-hour average isn't reached, there are still several hours per day where the ozone concentrations reach a threshold of "unhealthy for sensitive groups"

during a median 18-30 days each summer. As with the results in Table 1, there can be large variability from year to year, as the summer of 2017 shows that over half of the season had days with hourly ozone concentrations reaching 70 ppbv for sites QHW and MTMET, and had 12-20% of days reaching maximum hourly ozone concentrations into the "unhealthy for all" category (larger than 85 ppbv).

Table 1: Percentage of days (relative to the days sampled) per site per summer season where the daily maximum 8-hour ozone concentration surpassed the thresholds shown, with median percentages per site calculated from the yearly totals.

Site QBV	**Days Sampled**	**% ≥60 ppbv**	**% ≥65 ppbv**	**% ≥70 ppbv**	**% ≥85 ppbv**
2015	99	42.4	28.3	13.1	0.0
2016	106	34.9	14.2	7.5	0.0
2017	106	65.1	37.7	22.6	0.0
2018	106	58.5	33.0	13.2	0.9
2019	106	34.9	13.2	4.7	0.0
2020	106	34.0	17.0	11.3	0.0
Median	***106***	***37.3***	***21.7***	***11.8***	***0.0***
Site QHW	**Days Sampled**	**% ≥60 ppbv**	**% ≥65 ppbv**	**% ≥70 ppbv**	**% ≥85 ppbv**
2015	106	47.2	30.2	20.8	0.0
2016	101	29.7	16.8	10.9	0.0
2017	106	60.4	42.5	21.7	0.0
2018	104	51.0	26.9	11.5	1.0
2019	106	40.6	23.6	8.5	0.0
2020	103	35.9	21.4	12.6	0.0
Median	***105***	***44.3***	***25.2***	***11.9***	***0.0***
Site QRP	**Days Sampled**	**% ≥60 ppbv**	**% ≥65 ppbv**	**% ≥70 ppbv**	**% ≥85 ppbv**
2018	105	33.3	16.2	12.4	1.0
2019	106	60.4	40.6	22.6	0.9
2020	81	48.1	23.5	8.6	0.0
Median	***105***	***37.1***	***18.1***	***12.4***	***1.0***
Site MTMET	**Days Sampled**	**% ≥60 ppbv**	**% ≥65 ppbv**	**% ≥70 ppbv**	**% ≥85 ppbv**
2015	102	35.3	23.5	12.7	0.0
2016	106	23.6	14.2	6.6	0.0
2017	99	67.7	48.5	27.3	0.0
2018	79	81.0	55.7	32.9	1.3
2020	95	45.3	27.4	15.8	1.1
Median	***99***	***43.4***	***26.3***	***15.2***	***0.0***

Table 2: Percentage of days (relative to the days sampled) per site per summer season where the daily maximum 1-hour ozone concentration surpassed the thresholds shown, with median percentages per site calculated from the yearly totals.

Site QBV	**Days Sampled**	**% ≥60 ppbv**	**% ≥65 ppbv**	**% ≥70 ppbv**	**% ≥85 ppbv**
2015	99	59.6	46.5	34.3	11.1
2016	106	50.0	34.0	21.7	3.8
2017	106	84.0	67.0	44.3	12.3
2018	106	71.7	62.3	40.6	5.7
2019	106	50.0	37.7	23.6	2.8
2020	106	52.8	35.8	25.5	6.6
Median	***106***	***54.2***	***40.6***	***28.8***	***6.1***
Site QHW	**Days Sampled**	**% ≥60 ppbv**	**% ≥65 ppbv**	**% ≥70 ppbv**	**% ≥85 ppbv**
2015	106	65.1	53.8	32.1	11.3
2016	101	48.5	31.7	19.8	5.9
2017	106	77.4	67.9	52.8	15.1
2018	104	68.3	53.8	37.5	4.8
2019	106	62.3	41.5	26.4	1.9
2020	103	51.5	36.9	24.3	5.8
Median	***105***	***64.3***	***47.6***	***29.5***	***5.7***
Site QRP	**Days Sampled**	**% ≥60 ppbv**	**% ≥65 ppbv**	**% ≥70 ppbv**	**% ≥85 ppbv**
2018	105	72.4	57.1	44.8	8.6
2019	106	52.8	34.0	17.9	2.8
2020	81	61.7	44.4	25.9	9.9
Median	***105***	***53.3***	***34.3***	***20.0***	***7.6***
Site MTMET	**Days Sampled**	**% ≥60 ppbv**	**% ≥65 ppbv**	**% ≥70 ppbv**	**% ≥85 ppbv**
2015	102	63.7	44.1	29.4	7.8
2016	106	44.3	32.1	17.9	2.8
2017	99	82.8	69.7	57.6	19.2
2018	79	87.3	79.7	65.8	15.2
2020	95	58.9	50.5	32.6	9.5
Median	***99***	***65.7***	***48.5***	***31.3***	***9.1***

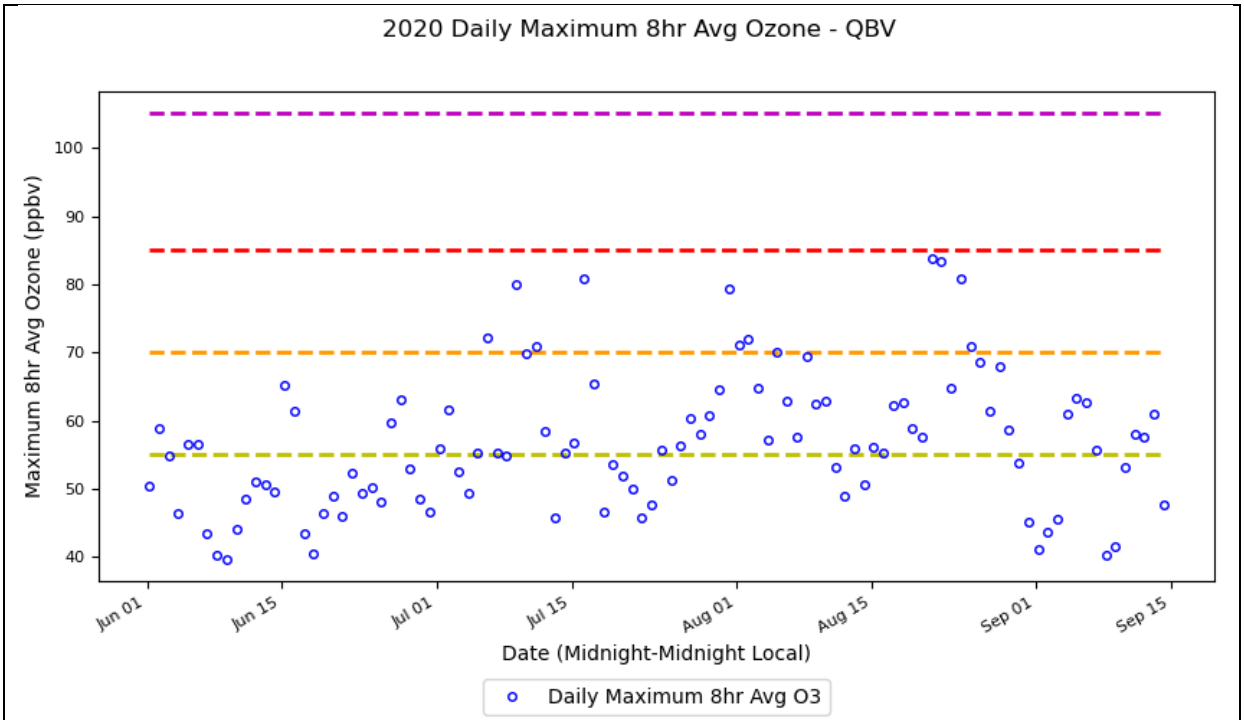

Figure 4: Daily maximum 8-hour average ozone concentrations (blue circles) for Bountiful (site QBV) calculated from 1 June - 15 September 2020. Dashed lines represent current NAAQS thresholds for moderate (>55 ppbv - yellow), unhealthy for sensitive groups (>70 - orange), unhealthy for all (>85 - red), and very unhealthy (>106 - magenta).

2. Results: Ozone Concentrations during 2021-2022 Summer Seasons

a) Introduction

The summer seasons of 2021 and 2022 were analyzed in more detail to (a) compare aggregate statistics with those provided for 2015-2020, (b) assess the evolution of specific high ozone case events in the Farmington Bay region with respect to meteorological conditions, and (c) delineate high ozone events where local and regional wildfire activity were present. Due to remaining concerns with coronavirus exposure, equipment deployment during summer 2021 was limited to placement of additional remote sensing and air quality equipment at existing sites. Considerable research equipment was deployed during summer 2022 for additional measurements of ozone concentrations and planetary boundary layer conditions.

b) Summer 2021 and 2022 Ozone Summary

The same data collection resources, averaging techniques, and occurrence tabulation methodologies used for the results in Section 2 were executed on data from the same sites for the two most recent summers. Table 3 depicts the percentage of days (1 June – 15 September) where 8-hour and 1-hour ozone concentrations eclipsed moderate, unhealthy for sensitive

groups, and unhealthy for all thresholds. The summer of 2021 produced more days with higher ozone concentrations compared to the median statistics from 2015-2020.

Table 3: Percentage of days (relative to the days sampled) from 1 June – 15 September 2021 where the daily maximum 8-hour and 1-hour ozone concentrations surpassed the thresholds shown, with median percentages per site calculated from the yearly totals.

8-Hour Average Ozone 2021					
Site ID	**Days Sampled**	**% ≥60 ppbv**	**% ≥65 ppbv**	**% ≥70 ppbv**	**% ≥85 ppbv**
QBV	106	67.9	47.2	22.6	0.9
QHW	106	67.9	46.2	21.7	1.9
QRP	106	60.4	40.6	22.6	0.9
MTMET	106	72.6	50.9	25.5	0.0
1-Hour Average Ozone 2021					
Site ID	**Days Sampled**	**% ≥60 ppbv**	**% ≥65 ppbv**	**% ≥70 ppbv**	**% ≥85 ppbv**
QBV	106	77.4	66.0	48.1	8.5
QHW	106	81.1	63.2	43.4	8.5
QRP	106	75.5	64.2	42.5	8.5
MTMET	106	84.0	67.0	53.8	10.4

Table 4 provides a similar summary for summer 2022. Statistically, the percentages of high ozone occurrence days for summer 2022 were closer to the median percentages shown above for 2015-2020. For example, site QBV recorded an 8-hour average concentration above 70 ppbv on 11.9% of assessed days during the 2022 study period (2015-2020 median was 11.8%).

Table 4: Percentage of days (relative to the days sampled) from 1 June – 15 September 2022 where the daily maximum 8-hour and 1-hour ozone concentrations surpassed the thresholds shown, with median percentages per site calculated from the yearly totals.

8-Hour Average Ozone 2022					
Site ID	**Days Sampled**	**% ≥60 ppbv**	**% ≥65 ppbv**	**% ≥70 ppbv**	**% ≥85 ppbv**
QBV	92	59.8	33.7	12.0	0.0
QHW	77	49.4	27.3	6.5	0.0
QRP	92	42.4	20.7	7.6	0.0
MTMET	92	30.4	12.0	4.3	0.0
1-Hour Average Ozone 2022					
Site ID	**Days Sampled**	**% ≥60 ppbv**	**% ≥65 ppbv**	**% ≥70 ppbv**	**% ≥85 ppbv**
QBV	92	78.3	58.7	38.0	5.4
QHW	77	66.2	55.8	40.3	6.5
QRP	92	65.2	45.7	32.6	6.5
MTMET	92	65.2	48.9	31.5	3.3

Figure 5 illustrates the influence of local and regional wildfires upon ozone concentrations based on simultaneous measurements of ozone, $PM_{2.5}$ and biomass black carbon concentrations at the MTMET site during both summers. As will be shown in Section 4, the impact of wildfires was much greater during the second half of summer 2021. Reviewing those data with respect to the ozone concentrations recorded at site MTMET, it was found that 61% of the days where the 8-hour average ozone concentration exceeded 65 ppbv also recorded $PM_{2.5}$ and black carbon concentration values that indicated the presence of wildfire smoke. Initial multi-day smoke episodes were detected from 10-16 July and 24-26 July, though all days with higher ozone concentrations during August and September 2021 occurred during the presence of wildfire smoke in the greater Wasatch Front region. A case study of the impacts of wildfire smoke on ozone concentration during August 6-8 2021 will be presented in Section 4. Compared to conditions during summer 2021, summer 2022 ozone concentrations were not heavily influenced by local and regional wildfire smoke. The only period where smoke appeared to have a larger influence on ozone concentrations in 2022 was from 7-12 September.

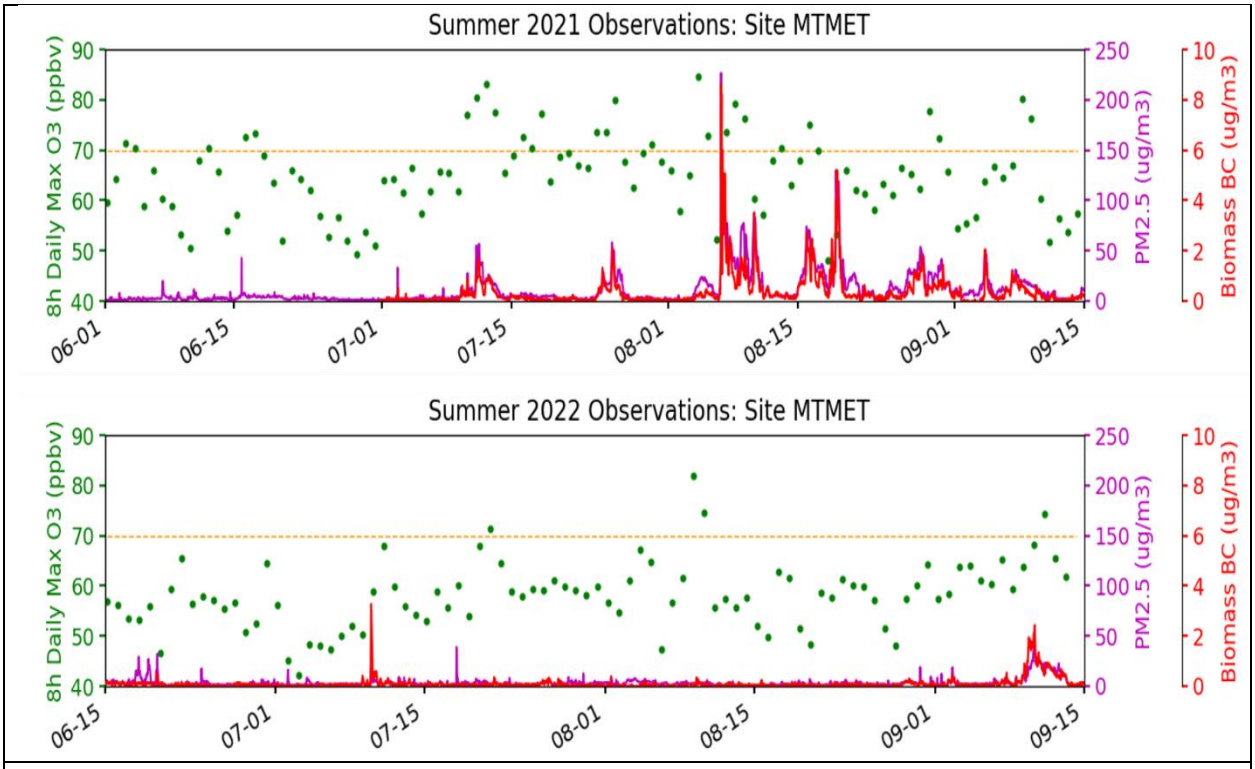

Figure 5. MTMET observations of 8h daily maximum O_3 (green dots), $PM_{2.5}$ (purple line), and biomass black carbon (red line) during summer 2021 (top) and summer 2022 (bottom) .

During summer 2022, ozone concentrations were collected and analyzed in greater detail from 10-12 permanent and field campaign sites in our region of interest. Figure 6 depicts, on a daily basis, how many of those reporting sites surpassed 8-hour and 1-hour average ozone

concentration thresholds for moderate (yellow), unhealthy for sensitive groups (orange), and unhealthy for all (red) categories.

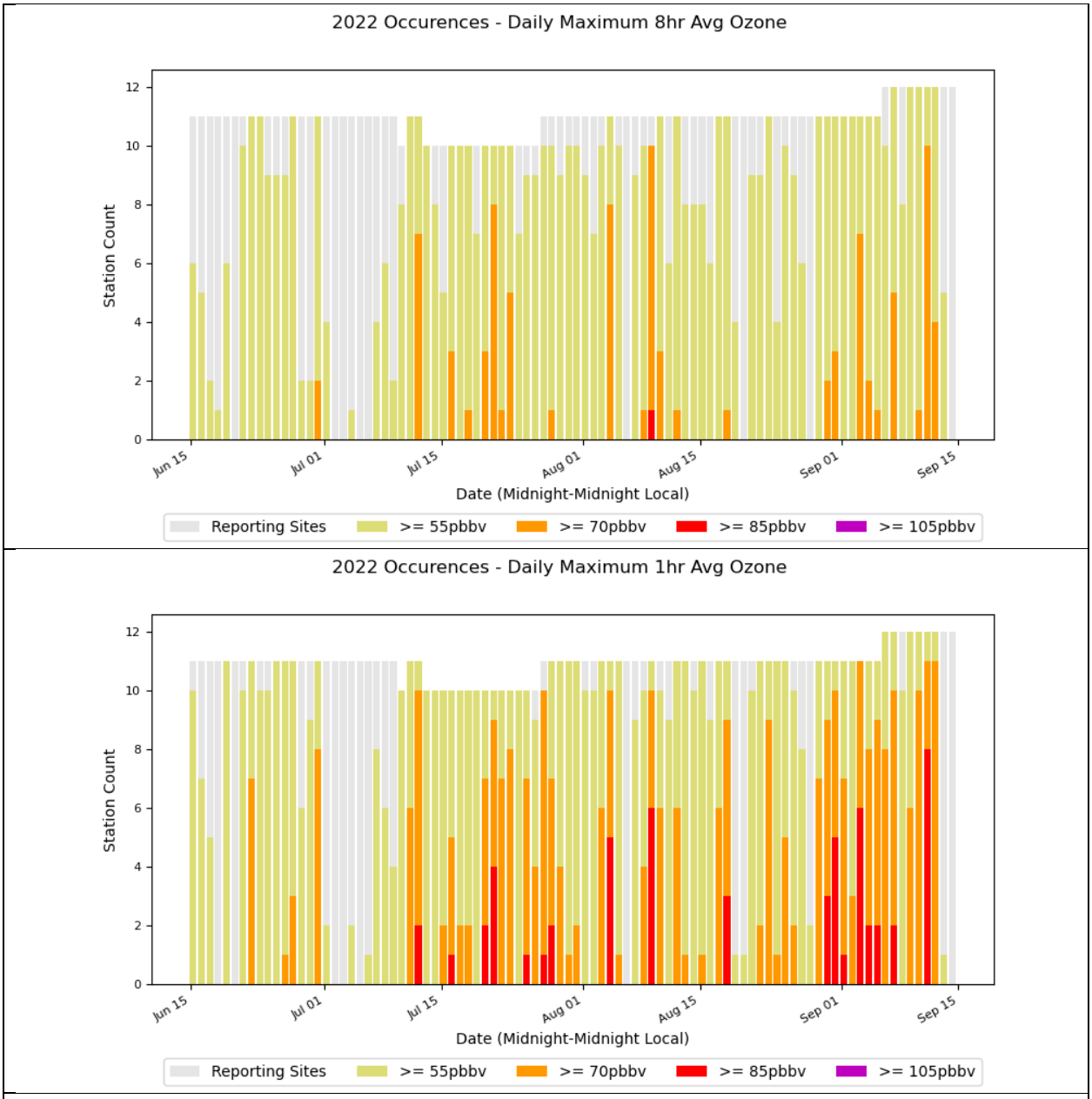

Figure 6: Count of reporting stations per day from 15 June - 15 September 2022 that exceeded maximum 8-hour (top) and 1-hour (bottom) average ozone concentrations for the thresholds defined in the legend below the graph.

Figure 6 highlights the multi-day episodic nature of these higher ozone occurrences during summer 2022. The first third of the study period (15 June – 15 July) only had two days with at least one site exceeding an 8-hour average of 70 ppbv. Meteorologically, much of this period was dominated with an unusually active weather pattern, with several periods of disturbances,

frontal passages, and strong synoptic flows influencing the region. This resulted in the majority of days only achieving maximum concentrations that were similar in magnitude to general "background" levels of ozone, which tend to be lower earlier in the summer. After mid-July the overall synoptic weather pattern shifted to a pattern more typical of mid-summer months, with summer monsoon influences taking hold later in the summer. Higher ozone days were seen more frequently in late July, a few shorter periods in August, and then an extended period in late August and early September.

Figure 7 provides a summary of ozone exceedances above selected thresholds for the entire period 2015-2022 in the Davis and Salt Lake County areas. The more "typical" conditions during summer 2022 are evident in contrast to the higher ozone concentrations in summer 2021 and 2017.

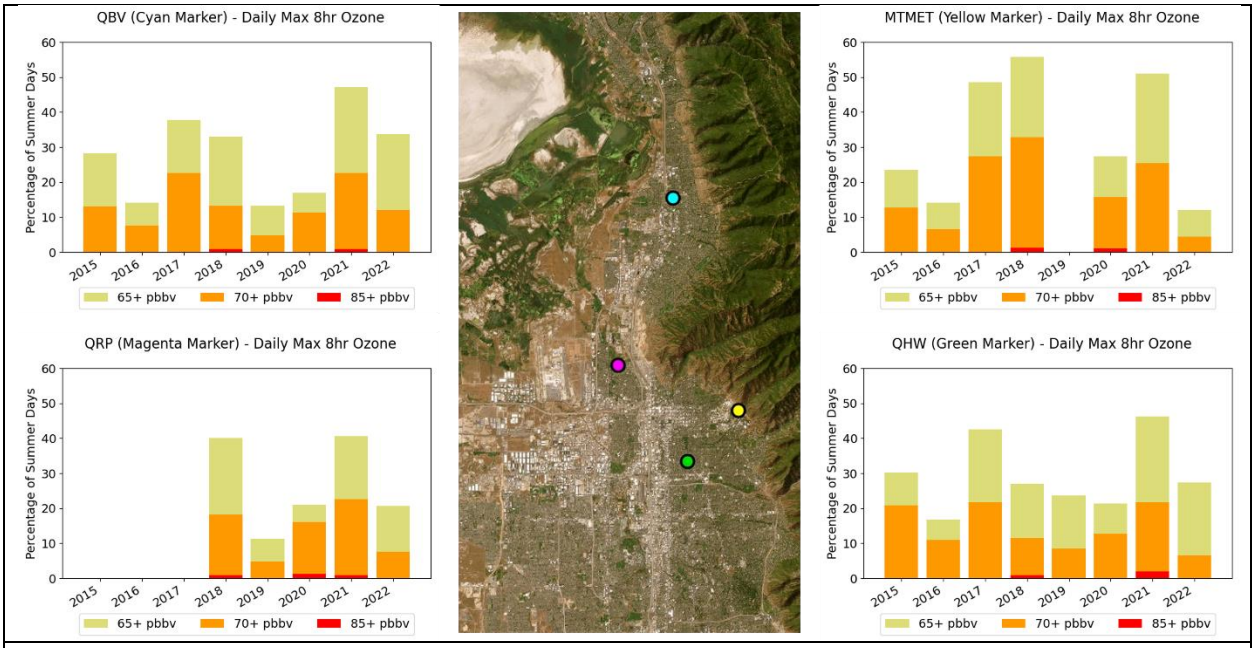

Figure 7: Percentage of summer days from 2015-2022 that exceeded maximum 8-hour average ozone concentrations for the thresholds defined in the legend below the graphs.

3. Summer 2022 Data Resources

In order to examine the meteorological conditions in the vicinity of Farmington Bay, we rely on the extensive networks of automated sensors that are available in the region (top panel of Figure 8). Data from these stations are available from Synoptic Data PBC or graphical displays from https://mesowest.utah.edu/. In addition, the twice-daily NWS rawinsonde launches provide critical temperature, moisture, and wind profiles through the boundary layer. Rawinsonde data and images are available from the University of Wyoming: https://weather.uwyo.edu/upperair/sounding.html.

Surface-based field instrumentation packages were deployed at selected locations during summer 2022 to augment DAQ and existing University of Utah sensor locations (bottom panel of Figure 8). As shown in the bottom panel of Figure 8, existing sites deployed by the University of Utah include those on campus (WBB and MTMET), at the Salt Lake landfill (USDR1), and at the entrance to the Antelope Island causeway (UUSYR). These were supplemented during summer 2022 by sensors located from south to north at UFD15/USDR5, USDR4, and UUPYA that were installed during the first part of June 2022. Sensors remain deployed during 2023 with the exception of the sodar at USDR5 and ozone sensor at UUPYA. These sites helped fill critical needs to sample meteorological conditions and ozone concentrations on the playa surfaces of Farmington Bay and adjacent wetlands. Table 5 summarizes site location information for stations referenced in this report. Table 6 provides a summary of measurement parameters collected at each station.

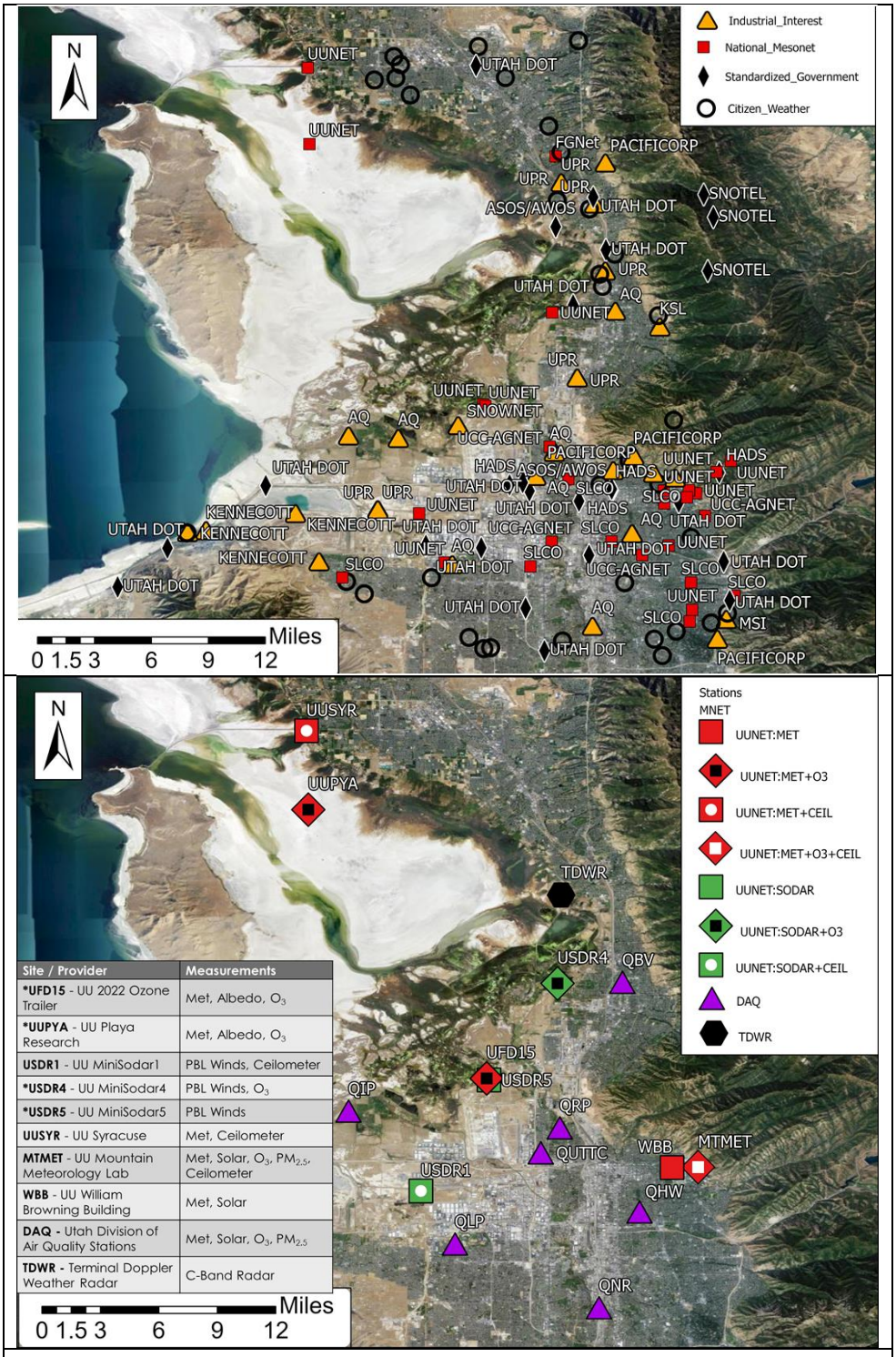

Site / Provider	Measurements
***UFD15** - UU 2022 Ozone Trailer	Met, Albedo, O_3
***UUPYA** - UU Playa Research	Met, Albedo, O_3
USDR1 - UU MiniSodar1	PBL Winds, Ceilometer
***USDR4** - UU MiniSodar4	PBL Winds, O_3
***USDR5** - UU MiniSodar5	PBL Winds
UUSYR - UU Syracuse	Met, Ceilometer
MTMET - UU Mountain Meteorology Lab	Met, Solar, O_3, $PM_{2.5}$, Ceilometer
WBB - UU William Browning Building	Met, Solar
DAQ - Utah Division of Air Quality Stations	Met, Solar, O_3, $PM_{2.5}$
TDWR - Terminal Doppler Weather Radar	C-Band Radar

Figure 8. Top: Ongoing meteorological observing sites. Bottom: Existing DAQ and university sites and additional sensors deployed at locations for this study.

Table 5: Summer 2022 Ozone Station Deployment Information Table						
2022 Ozone Instrumentation - University of Utah Mesonet (UUNET)						
Station ID - Name	**Latitude**	**Longitude**	**Elevation (ft)**	**Deployment Start**	**Deployment End**	**Site Description**
WBB – UU William Browning Building	40.766230	-111.84755	4728	1997-01-01 T00:00:00Z	ongoing	Urban, rooftop
MTMET – UU Mountain Meteorology Lab	40.766573	-111.82821	4993	2012-04-26 T00:00:00Z	ongoing	urban fringe, near grasslands, downslope from canyon
USDR1 – UU MiniSodar1	40.748950	-112.03392	5177	2013-07-23 T00:00:00Z	ongoing	Industrial, grassland, 200ft slope to the west
UUSYR – Syracuse	41.088470	-112.11880	4216	2017-03-17 T19:46:00Z	ongoing	urban fringe, grassland, remote
USDR4 – UU MiniSodar4	40.902080	-111.93253	4213	2022-06-07 T23:10:00Z	Sodar: ongoing Ozone: removed 2022-09-15	Industrial, grasslands, located at water treatment facility
UUPYA – UU Playa Research	41.030280	-112.11750	4987	2022-06-09 T02:13:00Z	Station: ongoing Ozone: removed 2022-09-12	Playa, evaporated lake bed, dirt/dust
UFD15 – UU 2022 Ozone Trailer	40.832010	-111.98509	4216	2022-06-15 T18:15:00Z	2022-09-12	Grassland, intermittent wetland, older playa
USDR5 – UU MiniSodar5	40.830855	-111.98339	4223	2022-06-23 T18:45:00Z	2022-09-12	Grassland, intermittent wetland, older playa

Table 6: Summer 2022 Ozone Station Measurement Parameters. Winds include wind speed and direction, Temp and RH include air temperature and relative humidity, pressure is local station pressure, and precipitation measured via tipping bucket rain gauge and/or weight based all-weather precipitation gauges filled with an antifreeze solution.

2022 Ozone Instrumentation - University of Utah MesoNet (UUNET)

Station Name	Air Quality	Boundary Layer	Meteorological	Radiation
WBB – UU William Browning Building	-	-	Wind, Temp, RH, Pressure, Precipitation	Shortwave: IN
MTMET – UU Mountain Meteorology Lab	Ozone, PM2.5, Black Carbon	Ceilometer	Wind, Temp, RH, Pressure, Precipitation	Shortwave: IN
USDR1 – UU MiniSodar1	-	Sodar	-	-
UUSYR – Syracuse	-	Ceilometer	Wind, Temp, Pressure	-
USDR4 – UU MiniSodar4	Ozone	Sodar	-	-
UUPYA – UU Playa Research	Ozone	-	Wind, Temp, RH, Pressure, Precipitation	Shortwave: IN & OUT UV: IN & OUT Longwave: IN & OUT
UFD15 – UU 2022 Ozone Trailer	Ozone	-	Wind, Temp, RH, Pressure	Shortwave: IN & OUT UV: IN & OUT
USDR5 – UU MiniSodar5	-	Sodar	-	-

UFD15 and USDR5 Sites

The trailer UFD15 was installed on a playa surface within the wetlands of the Rudy Duck Hunting Club (Figure 9). Surface meteorological weather sensors and a 2B 205 ozone concentration sensor were mounted on the trailer. Upward and downward pairs of Apogee shortwave and ultraviolet radiation sensors extended out over the reflective playa surface to provide quantitative assessment of surface shortwave and ultraviolet albedo. An Atmospheric Science Corporation (ASC) Mini-Sodar unit (USDR5), capable of sensing boundary layer winds in the lowest few hundred meters of the atmosphere, was located ~100 m from the trailer. Figure 10 illustrates a typical wind reversal at this site between 15-16 UTC (9-10 MDT) on 9 August 2022 from early morning offshore to late morning onshore flow.

Figure 9. Weather, radiation, and ozone sensors deployed with up/down pairs of radiation sensors viewing a playa surface within the wetlands of Farmington Bay. Sodar, USDR5, was located nearby. Undergraduates Alejandra Garcia, Sam Jurado (foreground), undergraduate Nicholas Buckley (left), staff Colin Johnson and graduate student Aaron McCutchan (background).

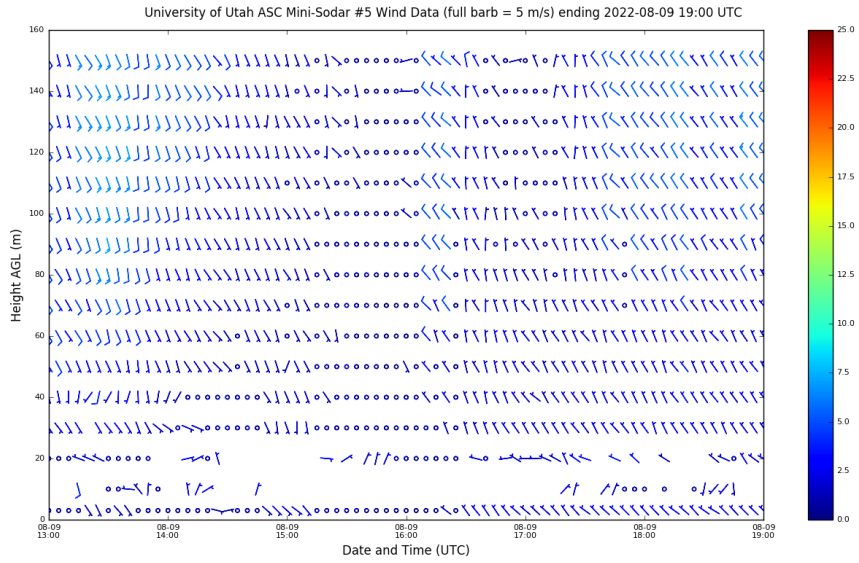

Figure 10. Boundary layer winds at USDR5 during the morning and afternoon of 9 August 2022 illustrating the wind reversal between 15-16 UTC from southerly (offshore) winds in the morning to northwesterly (onshore) winds in the afternoon.

USDR4 Site

Another ASC Mini-Sodar unit and 2B 205 ozone concentration sensor were placed at site USDR4 at the South Davis Water Treatment Plant immediately adjacent to Farmington Bay wetlands (Figure 11). This site was chosen to be close to the QBV DAQ site in order to evaluate typical conditions downwind of QBV during night and early morning hours and upwind of QBV during much of the day. Another aspect of this site is the likely local VOC emission resulting from water treatment processes (Byliński et al. 2019).

Figure 11. ASC mini-sodar located at USDR4. Similar sodars were in operation at USDR1 and USDR5.

UUPYA and UUSYR Sites

Figure 12. Location (star) of UUPYA site on the Farmington Bay playa.

In coordination with a NSF-funded research project focused on dust production from playa surfaces, extensive instrumentation was installed on a 10m tower at the UUPYA site. To support this project, a 2B 205 ozone sensor and upward and downward pairs of Apogee shortwave and ultraviolet radiation sensors were added. The radiation sensors provide surface shortwave and ultraviolet albedo representative of the highly reflective playa surfaces in Farmington Bay. In addition, a CL31 ceilometer was deployed at an existing University of Utah site in Syracuse (UUSYR) to be able to evaluate aerosol concentrations near the UUPYA site.

Figure 13. UUPYA tower on the Farmington Bay playa. Ozone and extensive meteorological sensors mounted on the tower.

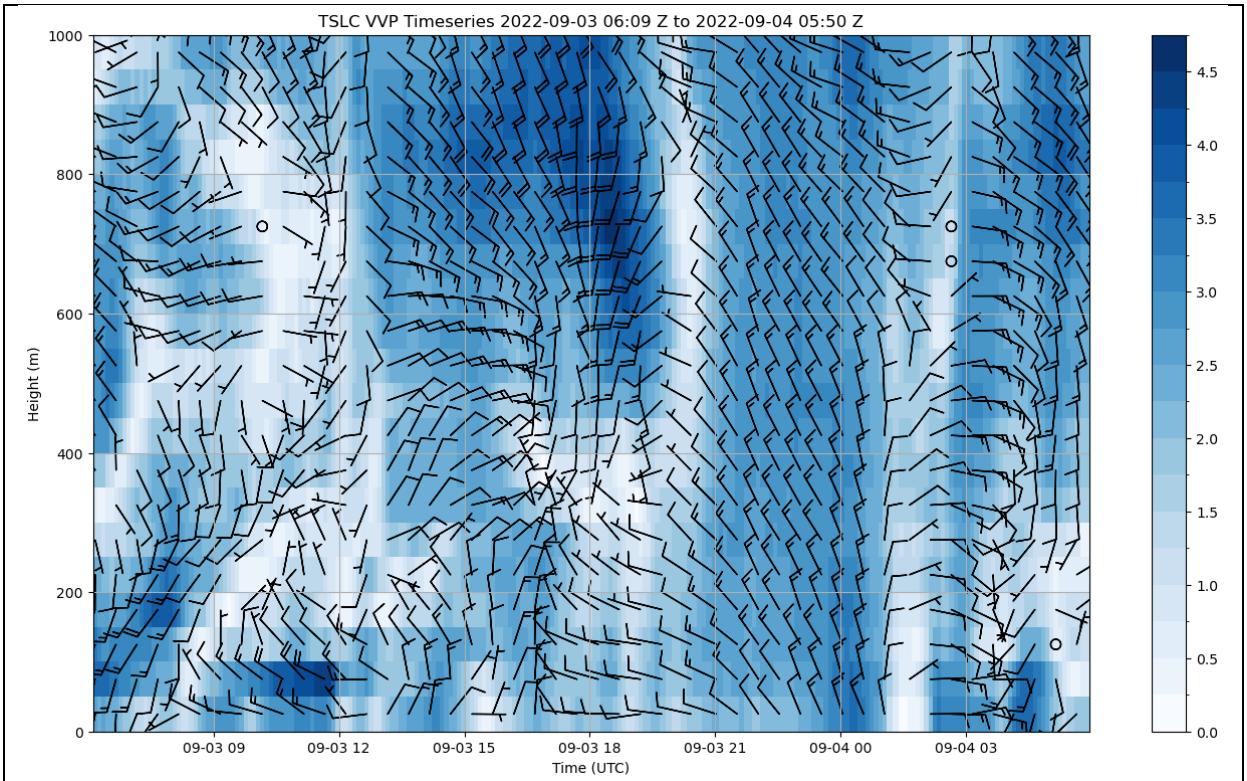

Figure 13. Wind speed (shading, m s^{-1}) and horizontal vector wind (wind barbs in m s^{-1}) during 6 UTC 3 Sep - 6 UTC 4 Sep 2022 in the lowest 1000 m from the TDWR north of the Salt Lake City Airport.

Terminal Doppler Weather Radar (TDWR)

Examination of boundary layer winds above Farmington Bay during summer 2022 is greatly aided by the TDWR radar installed directly north of the Salt Lake International Airport. The TDWR is used to detect hazardous low-level wind shear that affect plane landings and takeoffs. Data from the C-Band single-pol radar are accessible from cloud providers as part of the NOAA Open Data Program for the period from Aug 2020 to the present at volume scan intervals of 3 – 6 min and 150 m range resolution. Figure 13 illustrates the result of software developed by M.S. student Aaron McCutchan to monitor vertical wind profiles near the radar. Radial winds from scans at multiple elevation angles are available as shown in Figure 24.

CL-31 Ceilometers

CL-31 ceilometers that provide estimates of aerosol backscatter were deployed during the summer 2022 on the valley floor (USDR1), University of Utah campus on the east bench (MTMET), and near the Farmington Bay playa (UUSYR). In addition, aerosol backscatter data remains to be processed from the DAQ Hawthorne site (QHV). Daily time series of aerosol backscatter as a function of elevation are available at https://meso1.chpc.utah.edu/ceilometer/. For example, Figure 14 shows aerosol backscatter

from near the Farmington Bay playa (UUPYA) and southwest of the Salt Lake International Airport (USDR1) on 3 Sep 2022. The boundary layer depth is estimated to remain lower throughout the day at UUPYA compared to that evident south of Farmington Bay at USDR1. Note also the higher aerosol backscatter at UUPYA between 8-10 MDT compared to that at USDR1.

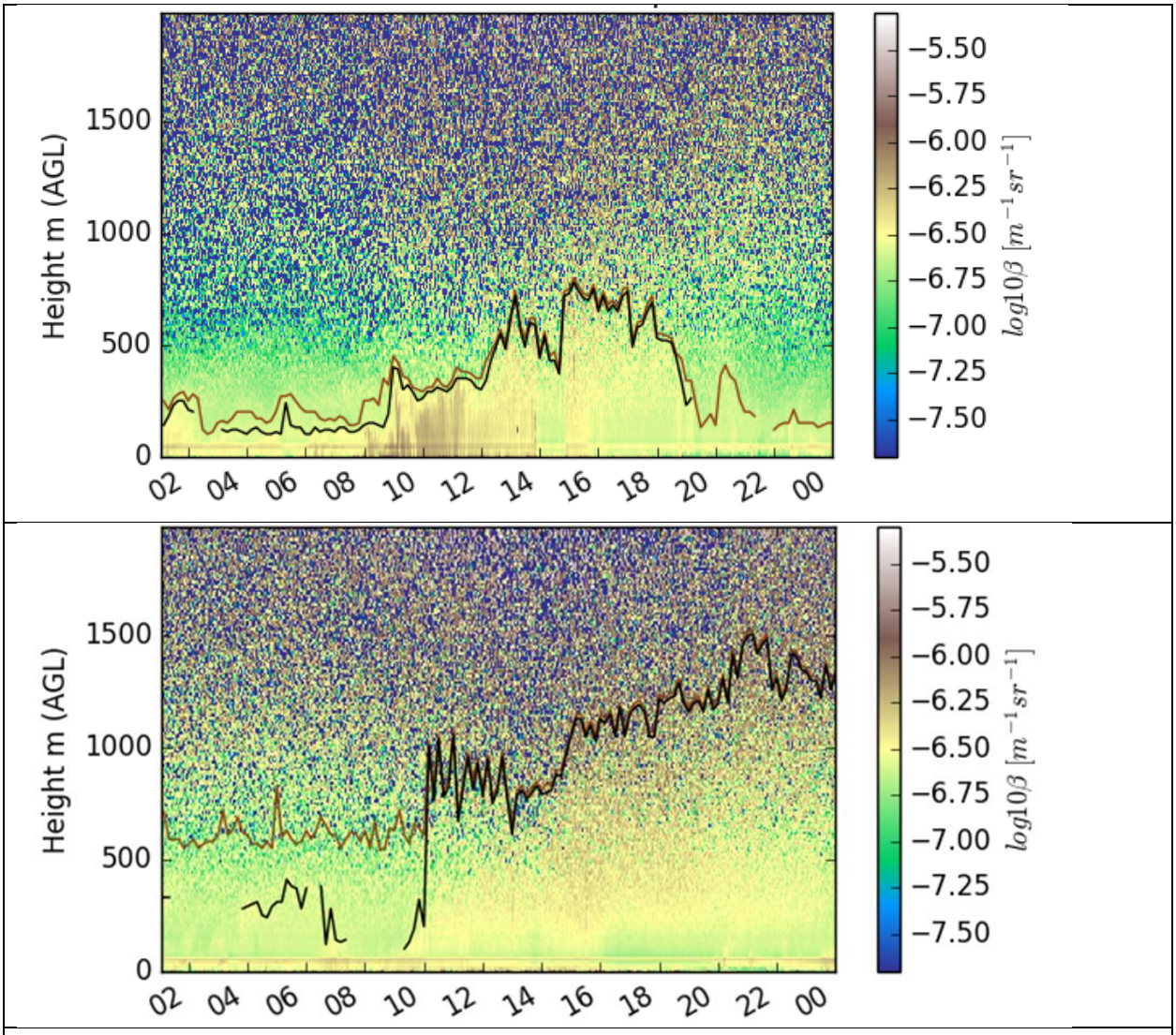

Figure 14. Aerosol backscatter from ceilometers at UUSYR (top) and USDR1 (bottom) on 3 Sep 2022.

Mobile Observations: KSL Helicopter and TRAX/E-BUS

$PM_{2.5}$ and ozone concentrations through the boundary layer are available when having the sensors onboard do not affect KSL helicopter operations (Crosman et al. 2017). During summer 2022, one or more flights are available on 36 days (Figure 15). For example, two flights (near noon and 6 PM local time) were available on 3 Sept 2022 (Figure 15). Displays of the KSL helicopter data are available from https://utahaq.chpc.utah.edu/. Additional mobile observations of $PM_{2.5}$ and ozone concentrations from sensors onboard three light rail cars and 1 E-BUS are also available during summer 2022 from the same link.

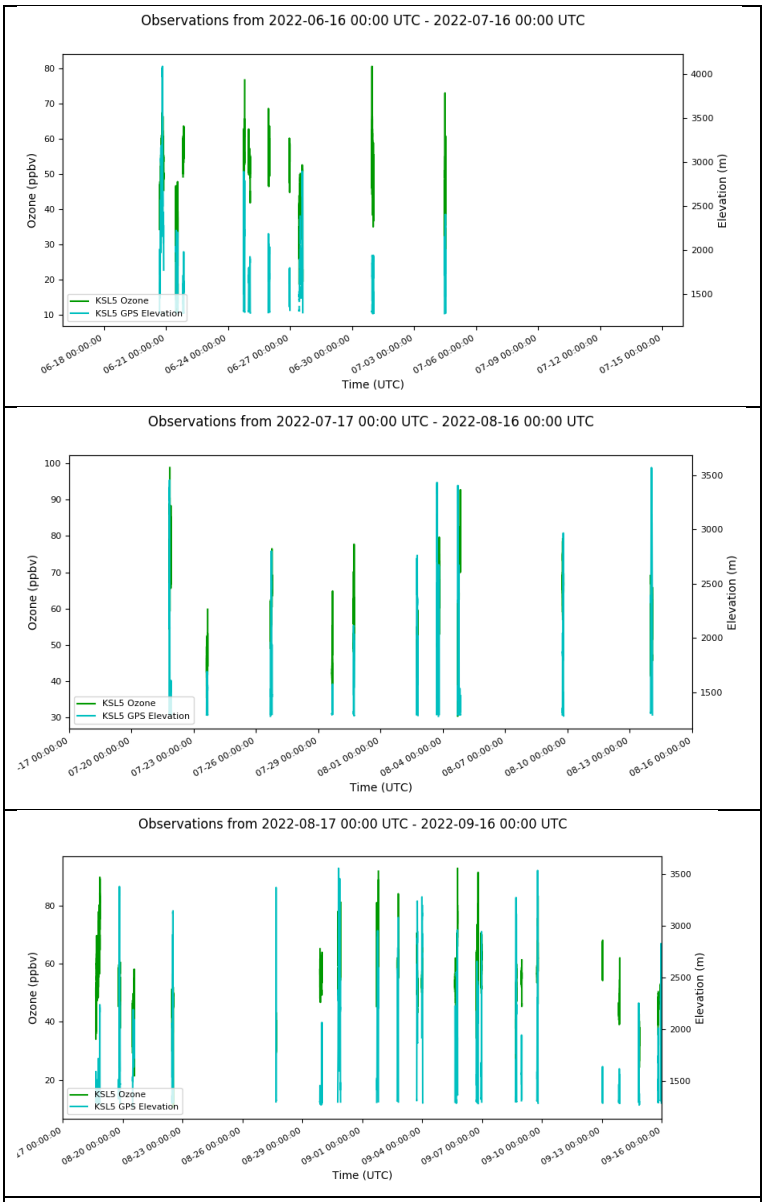

Figure 15. Vertical profiles of ozone concentrations (green lines) were available aloft from a sensor onboard the KSL traffic helicopter on 36 days during summer 2022.

High Resolution Rapid Refresh (HRRR) Analyses

We have available extensive capabilities to efficiently access and evaluate the analyses from the HRRR operational model (Blaylock et al. 2017b, 2018; Blaylock and Horel 2020; Gowan et al. 2022). Gowan et al. (2022) describe how the HRRR model output can be efficiently accessed at no cost now from the Amazon Web Services (AWS) Open Data program. HRRR model output is archived for both near-surface fields and for 3-dimensional fields both at pressure levels and in terrain following coordinates. As will be shown later, the HRRR operational model produces smoke products that capture the dominant features of large-scale smoke plumes. Beginning with the release of HRRRv4 in December 2020, the operational HRRR model has included a smoke tracer (primary PM2.5) and parameterizations of plume rise (Freitas et al. 2010) and satellite-derived fire radiative2 power (Ahmadov et al. 2017). Ye et al. (2021) summarize exhaustively the strengths and weaknesses of the HRRR approach to simulating smoke development and

transport in comparison to research models for the 2019 Williams, WA fire. Fotini et al. (2021) found that the HRRR model captured well the spread of dense smoke from California's 2018 Camp Fire during the early stages of the fire but later underestimated smoke concentrations due to underestimated satellite-derived fire radiative power.

The HRRR smoke-related products available at hourly temporal and 3-km spatial resolution across the contiguous U.S. during the summer seasons from 2021 to the present are:

- Near-surface (8 m) Smoke Mass Density (kg m^{-3})
- Total Column-Integrated Mass Density kg m^{-2})
- Fire Radiative Power (MW)

The lack of substantial wildfire impacts on ozone concentrations during summer 2022 reduced our reliance on HRRR analyses. We have relied on quick look displays to help evaluate flow features in the Farmington Bay region. For example, Figure 16 illustrates the down-valley to up-valley 10 m wind reversal between 1700 and 2000 UTC 3 Sep 2022 in the Salt Lake Valley from the HRRR.

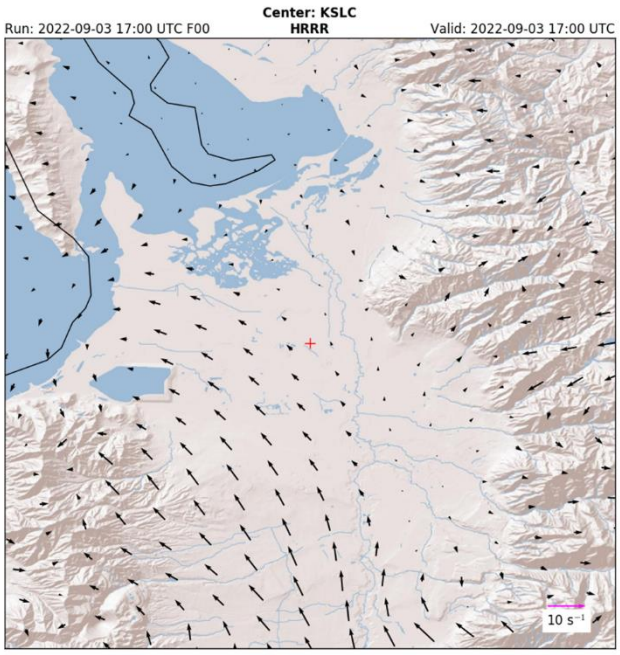

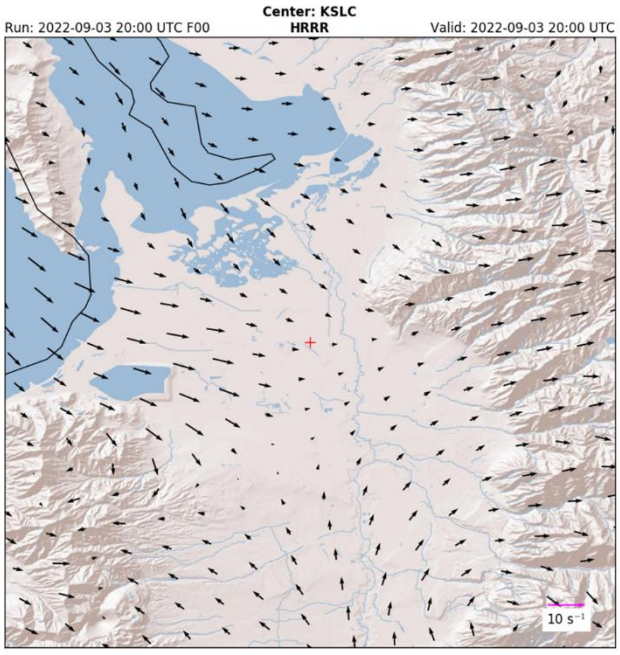

Figure 16. HRRR 10 m vector wind analyses (m s^{-1}) at 1700 and 2000 UTC 3 Sep 2022.

4. Results: Impacts of Wildfire Smoke on Ozone Concentrations

While the impact of wildfires on ozone production has been recognized for decades (Jaffe and Widge 2012), there is an increasing body of literature on the complex impacts of wildfires on ozone concentrations in urban areas. For example, Ninneman and Jaffe (2021) highlight that $P(O_3)$ on smoky days is largely driven by local photochemistry. They further postulate that a combination of anthropogenic VOC and NOx reductions would be more effective to decrease O_3 on smoke-free days while NOx reductions alone would be more effective on smoky days due to the high VOC levels present in smoke plumes. Wang et al. (2021) illustrate that vertical mixing and advection were major drivers of changes in surface ozone associated with wildfires in the southeastern U.S. Gao et al. (2020) describe more generally how aerosols weaken ozone photochemical production not only at the surface but also within the lower boundary layer leading to vertical ozone gradients that may result in higher amounts of ozone that can be later entrained back down towards the surface.

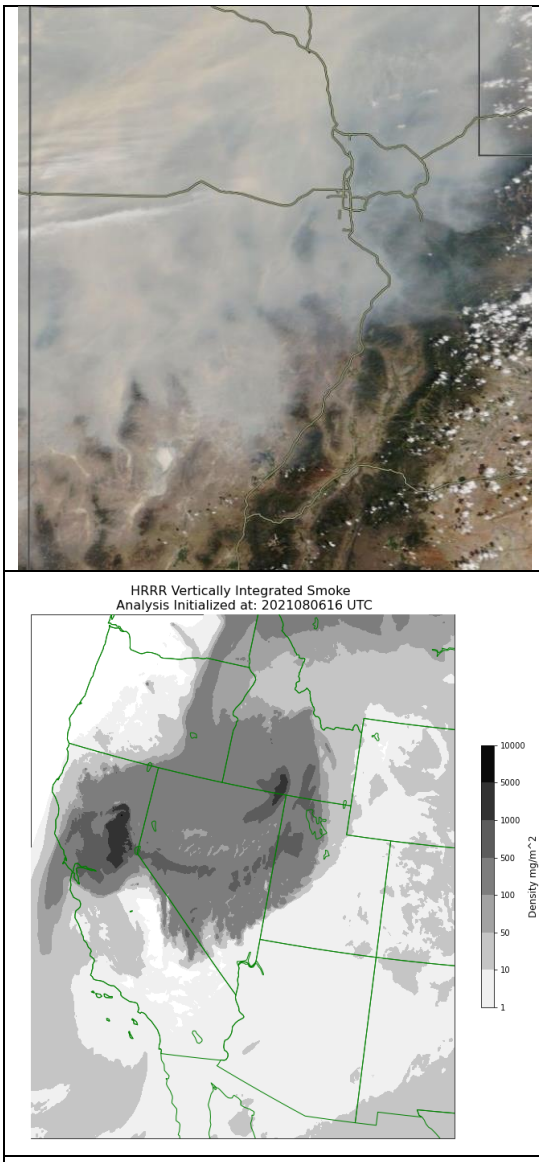

Figure 17. Dense smoke from the Dixie Fire on 6 Aug 2021 from: top- MODIS during the afternoon and bottom: HRRR vertically integrated smoke analysis at 16 UTC.

The impacts of wildfire smoke on ozone concentration are strikingly evident during the 5-7 Aug 2021 period in Davis and Salt Lake Counties. Figure 17 highlights the arrival of the dense smoke plume from the California Dixie Fire on 6 Aug 2021 on the basis of a MODIS satellite image during the afternoon and the operational High Resolution Rapid Refresh (HRRR) vertically-integrated smoke analysis at 16 UTC (10 MDT). Camera imagery confirms the rapid progression of the dense smoke plume across the Wasatch Front from 9-11 AM (not shown). As shown in Figure 18, the diurnal variations in Bountiful DAQ ozone (QBV) and $PM_{2.5}$ concentrations on the day before (5 Aug) are fairly typical for the summer with moderate ozone and $PM_{2.5}$ concentrations in the afternoon. As the smoke plume crossed Davis County, $PM_{2.5}$ at QBV spiked at 10 AM 6 Aug and $P(O_3)$ flattened during the rest of the morning when the largest increases typically occur. As smoke continued to blanket the Wasatch Front on 7 Aug, $PM_{2.5}$ concentrations remained elevated, ozone nocturnal titration was reduced, and ozone concentrations increased during the afternoon.

The suite of instrumentation near the mouth of Red Butte Canyon (MTMET) helps to illustrate in greater detail some of the processes underway during this period (Figure 19). As the smoke plume crossed the Wasatch Front, $PM_{2.5}$ and biomass black carbon concentrations spiked with incoming solar radiation reduced throughout the rest of the day leading to reduced $P(O_3)$. Reduced nighttime destruction of ozone arising from higher background ozone concentrations due to the Dixie Fire plume contributed to higher ozone concentrations on 7 Aug.

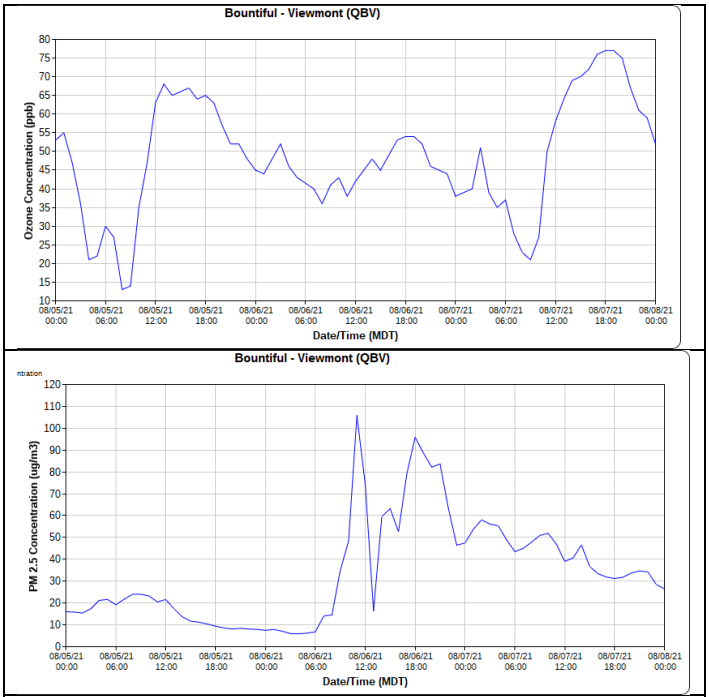

Figure 18. Ozone (top) and $PM_{2.5}$ (bottom) at Bountiful DAQ from 5-7 Aug 2021.

The interaction of the local meteorology on ozone concentrations during the entire 3-day period is illustrated in Figure 20. Note the transport of higher ozone concentrations from the Farmington Bay region into Davis County (QBV) due to the afternoon lake breeze and the nocturnal transport of low-moderate background concentrations from downslope winds at both QBV and MTMET.

Table 7 focuses on the 30 min when the smoke plume crossed MTMET and illustrates the obvious flattening of $P(O_3)$ as a result of the smoke shading. (Note: the values of $PM_{2.5}$ > 150 µg m^{-3} from the Met-One sensor at MTMET are likely an overestimate by as much as a factor of 2, a common deficiency for optical PM sensors, Delp and Singer 2020.)

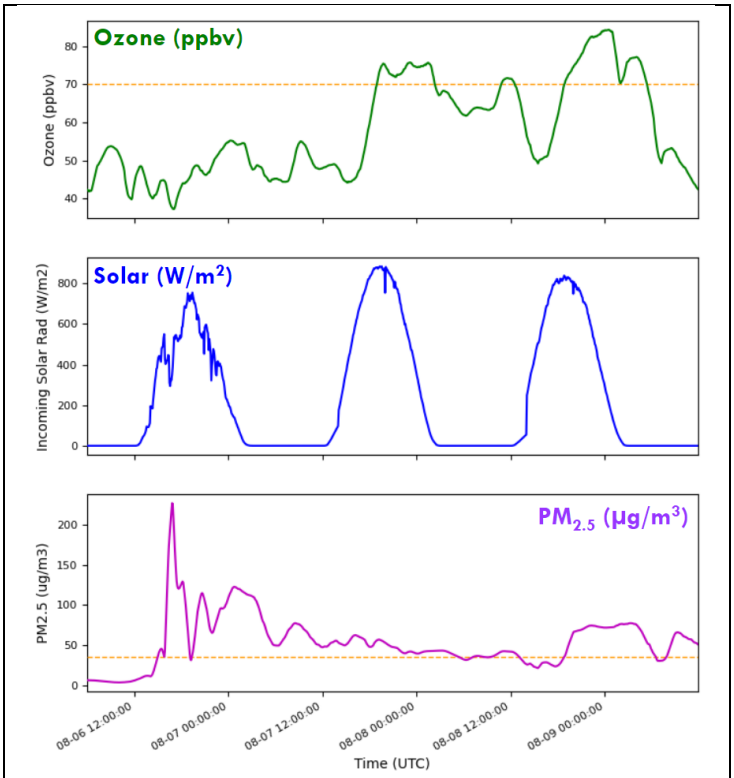

Figure 19. Ozone (top), incoming solar radiation (middle), and $PM_{2.5}$(bottom) at MTMET from 5-7 Aug 2021.

Table 7. Change in conditions between 9:45-10:15 MDT 6 Aug 2021 as the smoke plume crossed MTMET in the Salt Lake Valley

Time (MDT)	Solar (W m^{-2})	$PM_{2.5}$ (µg m^{-3})	BLK C (µg m^{-3})	Ozone (ppb)
9:45	533	9	0.1	42
9:50	550	9	0.0	41
9:55	427	132	.55	42
10:00	402	322	7.6	41
10:05	408	328	12.8	39
10:10	419	324	13.94	37
10:15	425	291	13.04	36

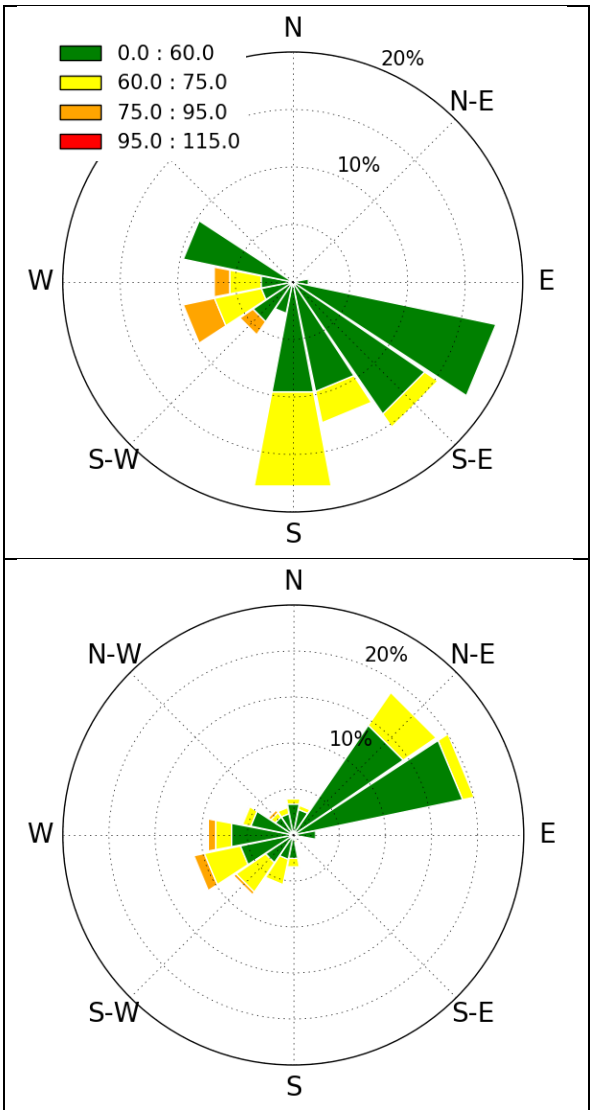

Figure 20. Ozone concentrations as a function of wind direction for the 3-day period 5-7 Aug 2021 at QBV (top) and MTMET (bottom).

Figures 17-20 and Table 7 illustrate the complex mix of meteorological and photochemical processes affecting ozone production along the Wasatch Front. Not surprisingly, the peak smoke concentration evident in Figure 21 at midnight 16 August 2021 in the Salt Lake Valley due to smoke drainage from the nearby Parley's Canyon fire was not captured at all by the HRRR near-surface or total column-integrated metrics (not shown). Both of those products simply depicted widespread light concentrations of smoke across Utah at that time. However, distinctive local smoke plumes present earlier that afternoon were evident in the HRRR analyses. Hence, establishing the extent to which the HRRR analyses are useful for local and remote sources of smoke needs to be assessed in greater detail than we have to date.

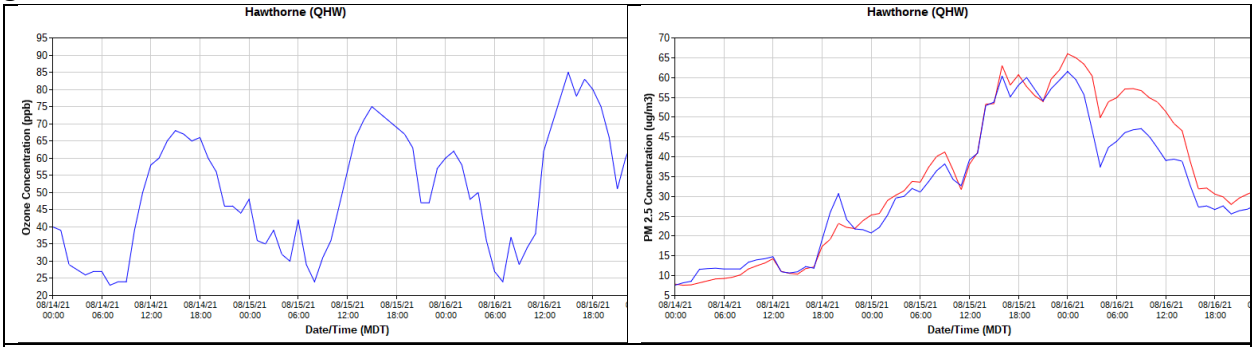

Figure 21. Ozone (left) and $PM_{2.5}$ (right) at Hawthorne DAQ from 14-16 Aug 2021. The Parley's Canyon fire started during the afternoon of the 14th.

5. Results: High Ozone Concentration Case Studies

Figure 22 highlights the increase in ozone concentrations during the five days with highest peak ozone concentrations at each of the sites near Farmington Bay. While all four sites have substantive ozone titration prior to sunrise, the lowest ozone concentrations at sunrise are at USDR4 and highest are at the Bountiful DAQ site (QBV). The former may result from the abundance of VOCs immediately upstream from the Davis water treatment facility and the latter may be due to downslope transport of background ozone concentrations. High ozone production rates, $P(O_3)$, are evident during all of these mornings with slight differences as to when the peak concentrations occur. As a general rule, peak concentrations are observed roughly an hour later at QBV than at the other sites, which could result in part from the hourly time averaging for QBV.

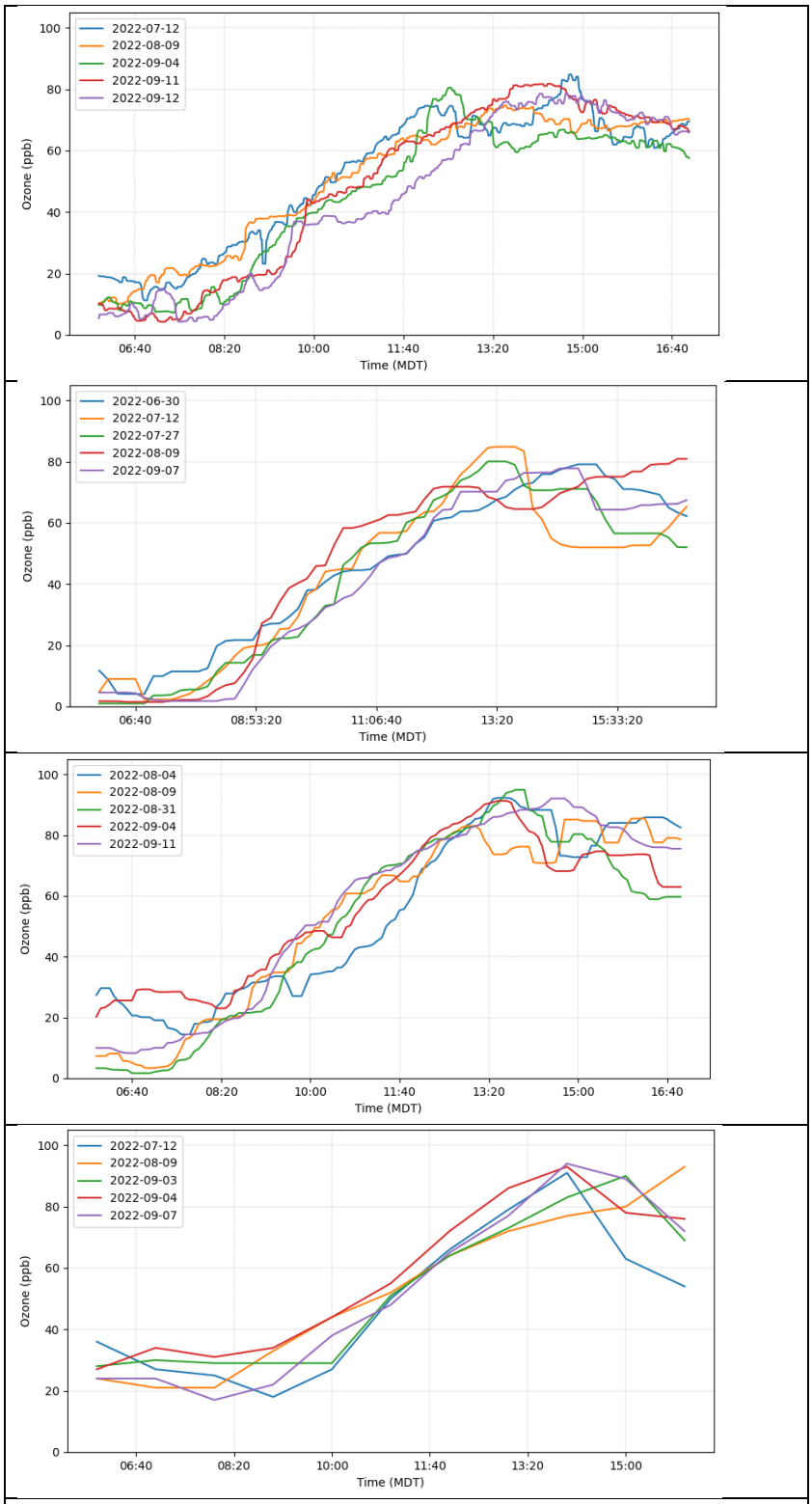

Figure 22. Ozone concentrations during the 5 days with the highest maximum O_3 concentration at: (a) UUPYA; (b) USDR4; (c) UFD15 and (d) QBV.

The upper panel of Figure 23 overlays the ozone concentrations at 5 sites in northern Salt Lake and Davis Counties on 9 Aug 2022, a day with some of the highest ozone concentrations observed during the summer (Figure 22). On this day, northern Utah was

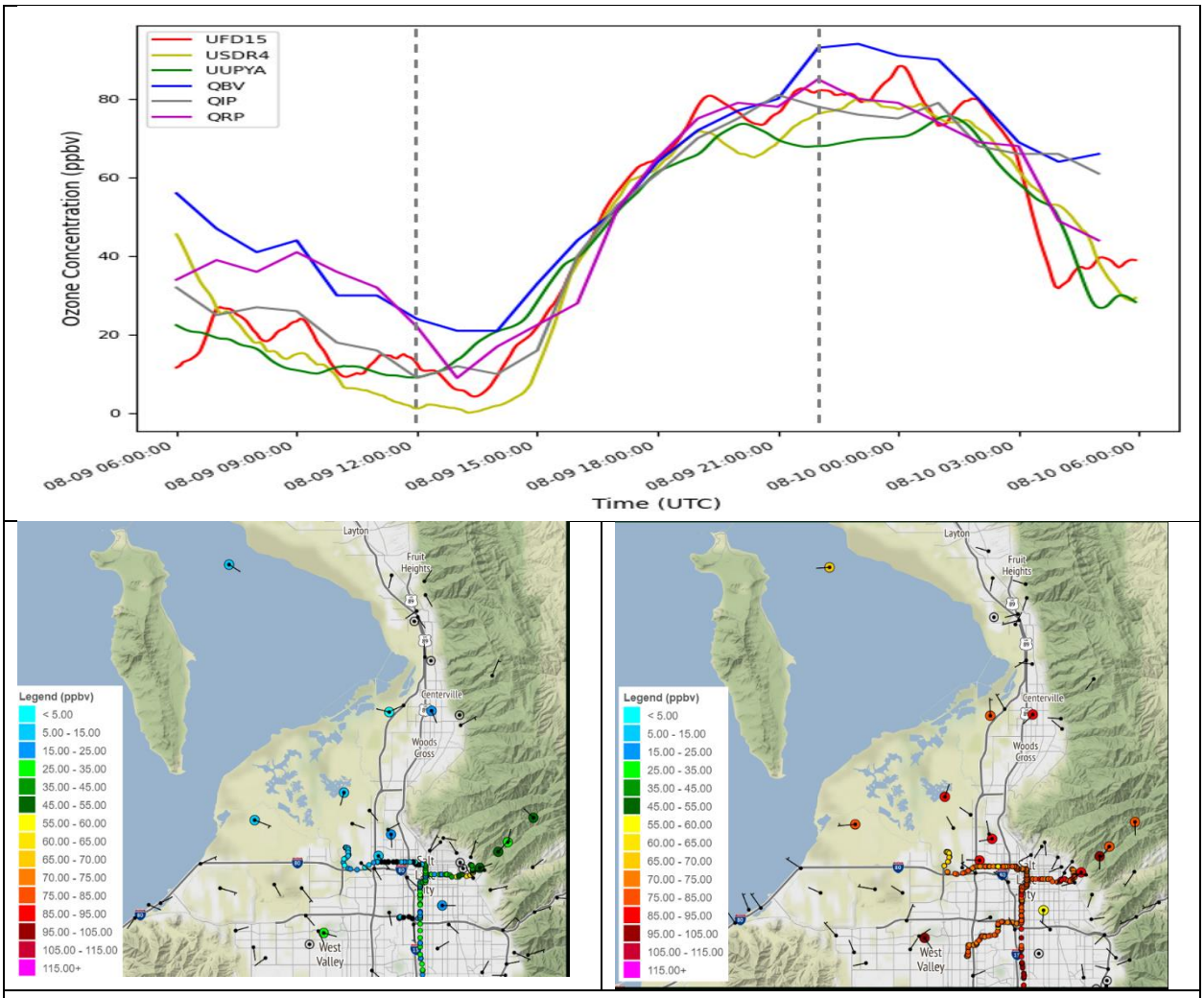

Figure 23. Top: Evolution of ozone concentrations on 9 Aug 2022 at 6 sites in northern Salt Lake and Davis Counties. Bottom left: Wind speed (m s^{-1}) and direction and ozone at 12 UTC (6 MDT). Bottom right: As in the left panel except for 22 UTC (16 MDT). Full barbs denote 2 m s^{-1}.

on the western edge of an upper level ridge that suppressed monsoon moisture from reaching the area. Afternoon temperatures were very high reaching 37.2°C at the Salt Lake City Airport (KSLC) and surface winds were driven by local thermally-driven flows due to terrain and Lake. The lower panels illustrate the availability of ozone observations from mobile light rail cars as well as the available fixed sites at 6 MDT (left panel) and 22 MDT (right panel) respectively. Morning concentrations on and near Farmington Bay tend to be lower than those in the urban Salt Lake Valley. The ozone production rate is high at all locations, but peak concentrations tend to be lower over the playa and in the wetland regions (UUPYA, UFD15, USDR4, QIP) relative to the higher peak at Bountiful (QBV).

The onset of lake breeze flows during 3 Sept 2022 are shown in Figure 24. At 11 MDT (17 UTC), southerly down valley near-surface flows and low ozone concentrations are evident before the development of the lake breeze originating over Gilbert Bay. Wind confluence over the

southern playa surfaces and wetlands of Farmington Bay is evident in the radial winds from the TDWR radar at this time with northerly winds in the north and southerly flow in the south. Such flow would tend to concentrate precursor chemicals in this region and possibly lead to enhanced ozone production rates. Three hours later (14 MDT), northwesterly flows from Gilbert Bay impinge on the northern end of the Salt Lake Valley and northerly flows extend across the Salt Lake City Airport from Farmington Bay. The large arrows in Figure 24 help to illustrate the radial wind directions that define the critical flow features during this period.

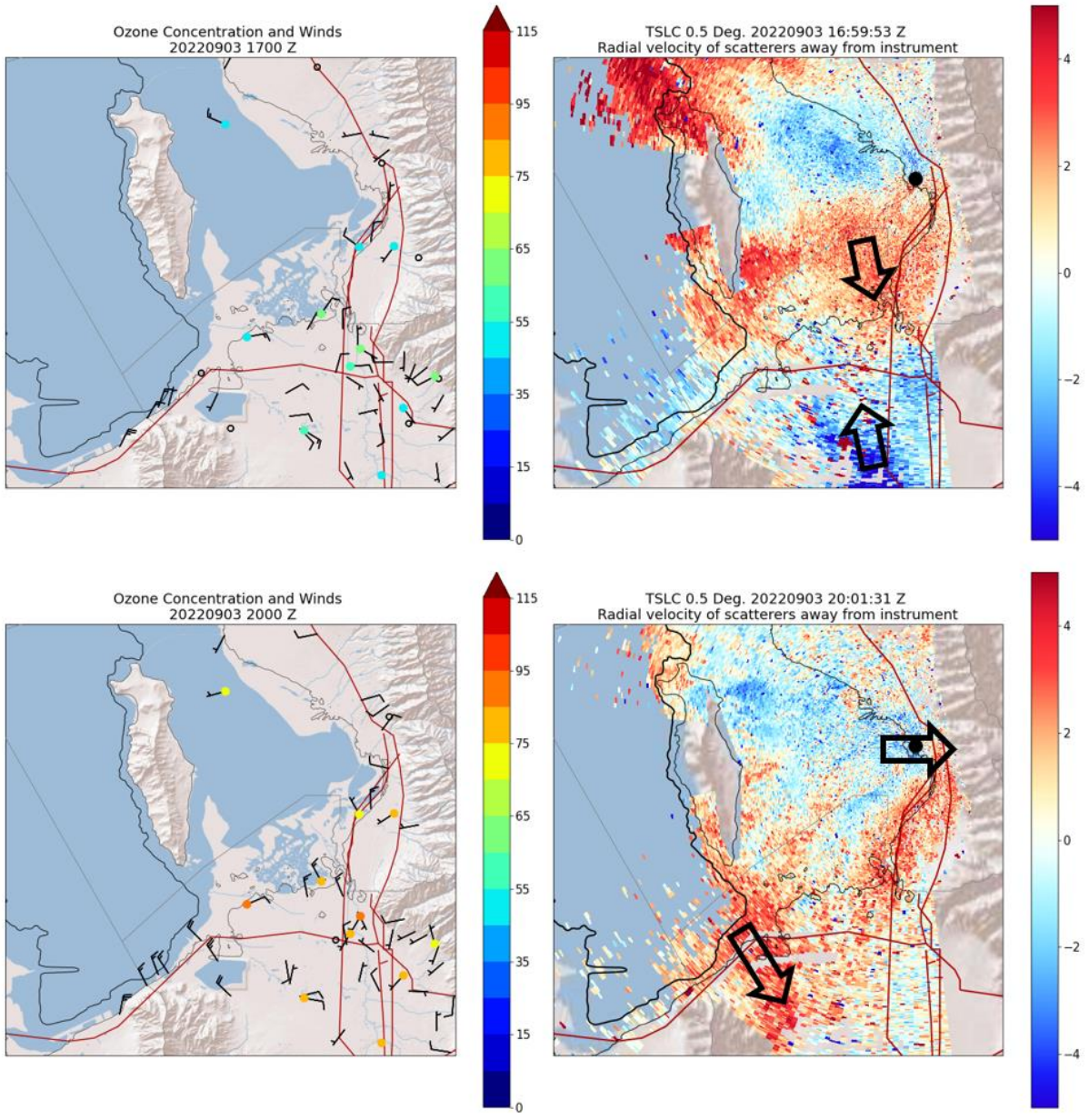

Figure 24. Top left: Ozone concentrations and wind at 17 UTC (11 MDT) 3 Sep 2022. Top right: Radial wind speeds from the TDWR at 0.5° scan angle at 17 UTC. Lower left: As in the top left except for 20 UTC (14 MDT). Lower right: As in the top right except for 20 UTC.

6. Results: Impacts of Surface Reflectance on Ozone Production

Based on the needs expressed by DAQ modelers, we purchased and installed two pairs of UV-A radiation sensors (300-400 nm) from Apogee Instruments: at the playa (UUPYA) and wetland playa (UFD15) sites. Underestimates of ozone production identified in recent DAQ simulations were thought to possibly result from underestimating the albedo of high-intensity UV-A radiation. As expected, the UUPYA had higher UV-A albedo due to increased reflectance from the exposed soil surface (see Figure 25). The soil type at UFD15 had higher amounts of clay leading to lower albedo during the summer than at UUPYA.

Notable in Figure 25 is the extent to which albedo estimates for UV or total shortwave exhibit similar trends over the summer. Hence, since total shortwave albedo is more commonly observed, it may be less critical to deploy additional sensors to measure UV albedo. However, additional work should be done to assess the extent to which the reduced UV albedo relative to shortwave albedo is independent of soil type.

Also evident in Figure 25 is the anticipated high sensitivity of albedo to surface wetness and soil type of playa surfaces (Craft and Horel 2019). The camera and MODIS imagery in Figure 25 for conditions before and after measurable precipitation provide the context for the sharp drop in albedo at UUPYA between 11 and 17 July 2020. The smaller drop in albedo at UFD15 likely results from the originally darker surface due to the higher clay content of the soil.

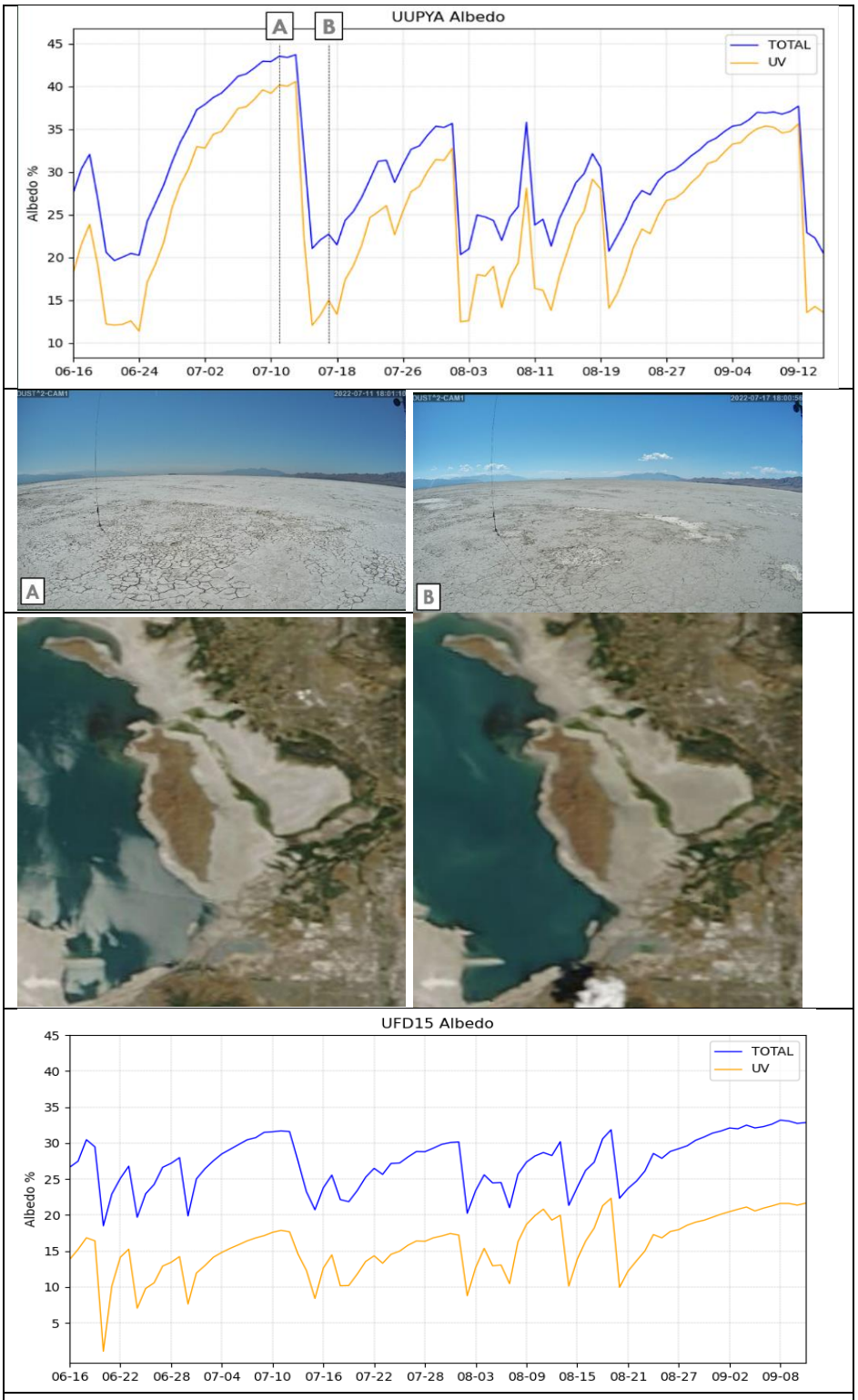

Figure 25. Shortwave (Total) and ultraviolet (UV) albedo at UUPYA (top) and UFD15 (bottom). Middle frames: Camera and MODIS images before and after mid-July rain event.

7. Recommendations

The data and results from this study should be of great utility for planning future studies of summer ozone along the Wasatch Front. We have demonstrated the utility of the image processing required to utilize the images from the operational Terminal Doppler Weather Radar and research deployments of surface based remote sensors (sodars, ceilometers) to examine the impacts of complex boundary layer flows on transport of chemical species affecting ozone along the Wasatch Front.

Future field programs intended to inform State Implementation Plans required for ozone exceedances along the Wasatch Front should recognize the need to monitor conditions continuously throughout the summer season, and also during intensive field periods that take advantage of a range of instrumentation. The interplay between emission sources and photochemical production and destruction of ozone is modulated extensively by a rich mix of boundary layer processes spanning a wide range of temporal and spatial scales. Considerable in-situ and remote observational assets are available that can be used to understand the coupling between atmospheric conditions and chemical processes and to initialize and validate models used to test strategies required for State Implementation Plans.

8. Data Management

Extensive amounts of publicly-accessible provisional data, quality-controlled data, and figures generated as part of this project are available via: https://home.chpc.utah.edu/~u1375211/o3_2022/. Our archive will be maintained and developed further over the next several years as we intend to continue analyzing data resulting from this project. For example, comma-delimited files for each sodar are available now at 15 minute time resolution here: https://home.chpc.utah.edu/~u1375211/o3_2022/data/sodar_data/_Processed/2022_Processed/. Images are available to assess sodar data quality as well: https://home.chpc.utah.edu/~u1426024/SODAR/

References

Ahmadov, R., and Coauthors, 2017: Using VIIRS fire radiative power data to simulate biomass burning emissions, plume rise and smoke transport in a real-time air quality modeling system. 2017 IEEE International Geoscience and Remote Sensing Symposium (IGARSS), 2806–2808.

Blaylock, B., J. Horel, E. Crosman, 2017a: Impact of Lake Breezes on Summer Ozone Concentrations in the Salt Lake Valley. *J. Appl. Meteor. Clim.*56, 353-370. http://journals.ametsoc.org/doi/abs/10.1175/JAMC-D-16-0216.1

Blaylock, B., J. Horel, S. Liston, 2017b: Cloud archiving and data mining of High Resolution Rapid Refresh Model Output. *Computers and Geosciences*, 109, 43-50. doi.org/10.1016/j.cageo.2017.08.005

Blaylock, B., J. Horel, C. Galli, 2018: High-Resolution Rapid Refresh Model Data Analytics Derived on the Open Science Grid to Assist Wildfire Weather Assessment. *Journal of Atmospheric and Oceanic Technology,* 35*,* 2213-2227. https://journals.ametsoc.org/doi/abs/10.1175/JTECH-D-18-0073.1

Blaylock, B., J. Horel, 2020: Comparison of Lightning Forecasts from the High-Resolution Rapid Refresh Model to Geostationary Lightning Mapper Observations. *Wea. Forecasting.* 35, 401-416. https://journals.ametsoc.org/doi/abs/10.1175/WAF-D-19-0141.1

Byliński, H., J. Gębicki, and J. Namieśnik1, 2019: Evaluation of Health Hazard Due to Emission of Volatile Organic Compounds from Various Processing Units of Wastewater Treatment Plant*. Int J Environ Res Public Health*. 2019 May; 16(10): 1712. doi: 10.3390/ijerph16101712

Craft, K., J. Horel, 2019: Variations in surface albedo arising from flooding and dessication cycles on the Bonneville Salt Flats, Utah. J. Appl. Meteor. Clim., 58. 773-785. https://journals.ametsoc.org/doi/ full/10.1175/JAMC-D-18-0219.1

Crosman, E., A. Jacques, J. Horel, 2017: A Novel Approach for Monitoring Vertical Profiles of Boundary-Layer Pollutants: Utilizing Routine News Helicopter Flights. *Atmospheric Pollution Research.* 8, 828-835. http://dx.doi.org/10.1016/j.apr.2017.01.013

Delp, W, and B. Singer, 2020: Wildfire Smoke Adjustment Factors for Low-Cost and Professional PM2.5 Monitors with Optical Sensors. *Sensors,* **20,** 3683; doi:10.3390/s20133683

Fotini, K. and coauthors, 2022: High-resolution smoke forecasting for the 2018 Camp Fire in California. *Bull. Amer. Met. Soc*. In Press. DOI: https://doi.org/10.1175/BAMS-D-20-0329.1

Freitas, S. R., K. M. Longo, J. Trentmann, and D. Latham, 2010: Technical Note: Sensitivity of 1-D smoke plume rise models to the inclusion of environmental wind drag. *Atmospheric Chemistry and Physics*, **10** (2), 585–594, doi:https://doi.org/10.5194/acp-10-585-2010, https://acp.copernicus.org/articles/10/585/2010/

Gao, J. Y. Li, B. Zhu, B. Hu, L. Wang, and F. Bao, 2020: What have we missed when studying the impact of aerosols on surface ozone via changing photolysis rates? Atmos. Chem. Phys., 20, 10831–10844, 2020. https://doi.org/10.5194/acp-20-10831-2020

Gowan, T. A., J. Horel, A. Jacques, 2022: Using cloud computing to analyze model output archived in ZARR format. *Journal of Atmospheric and Oceanic Technology.* DOI: 10.1175/JTECH-D-21-0106.1

Horel, J., E. Crosman, R. Martin, J. Sohl, S. Arens, 2016a: *2015 Great Salt Lake Summer Ozone Study.* Final Report to the Utah Division of Air Quality. 38 pp.

Horel, J., E. Crosman, A. Jacques, B. Blaylock, S. Arens, A. Long, J. Sohl, R. Martin, 2016b: Influence of the Great Salt Lake on summer air quality over nearby urban areas. *Atmospheric Science Letters*, **17**, 480-486. doi: 10.1002/asl.680

Jaffe, D.A., and Wigder, N.L., 2012. Ozone production from wildfires: A critical review. Atmospheric Environment 51, 1–10, doi:10.1016/j.atmosenv.2011.11.063.

Long, A., 2016: *Analysis of summer ozone concentration in the salt lake valley*. M.S. thesis. University of Utah. 83pp

Ninneman M., D. Jaffe, 2021: The impact of wildfire smoke on ozone production in an urban area: Insights from field observations and photochemical box modeling, Atmospheric Environment 267 (2021) 118764. https://doi.org/10.1016/j.atmosenv.2021.118764

Searer, A., N. Gabriel, John Horel, 2022: Impact of Lake Breezes on Ozone Concentrations Near The Great Salt Lake from 2015-2020. *2022 AMS Student Conference.* https://ams.confex.com/ams/102ANNUAL/meetingapp.cgi/Paper/397748

Wang, B., Kuang, S., Pfister, G. G., Pour-Biazar, A., Buchholz, R. R., Langford, A. O., & Newchurch, M. J. (2021). Impact of the 2016 Southeastern US Wildfires on the vertical distribution of ozone and aerosol at Huntsville, Alabama. Journal of Geophysical Research: Atmospheres, 126, e2021JD034796. https://doi.org/10.1029/2021JD034796

Ye, X., and coauthors, 2021: Evaluation and intercomparison of wildfire smoke forecasts from multiple modeling systems for the 2019 Williams Flats fire. Atmos. Chem. Phys., 21, 14427–14469, 2021 https://doi.org/10.5194/acp-21-14427-2021